Accepted Manuscript

Hydrogeochemical and stable isotope data of Groundwater of a multi-aquifer system: Northern Gafsa basin - Central Tunisia

Naziha Mokadem, Abedslem Demdoum, Younes Hamed, Salem Bouri, Rihab Hadji, Adrian Boyce, Rabah Laouar, Abedaziz Sâad

PII: S1464-343X(15)30105-9

DOI: 10.1016/j.jafrearsci.2015.11.010

Reference: AES 2414

To appear in: *Journal of African Earth Sciences*

Received Date: 11 April 2014

Revised Date: 7 November 2015

Accepted Date: 9 November 2015

Please cite this article as: Mokadem, N., Demdoum, A., Hamed, Y., Bouri, S., Hadji, R., Boyce, A., Laouar, R., Sâad, A., Hydrogeochemical and stable isotope data of Groundwater of a multi-aquifer system: Northern Gafsa basin - Central Tunisia, *Journal of African Earth Sciences* (2015), doi: 10.1016/j.jafrearsci.2015.11.010.

Hydrogeochemical and stable isotope data of Groundwater of a multi-aquifer system: Northern Gafsa basin - Central Tunisia

Naziha Mokadem[a], Abedslem Demdoum[b], Younes Hamed[a,c], Salem Bouri[a], Rihab Hadji[b], Adrian Boyce[d], Rabah Laouar[e], Abedaziz Sâad[f]

[a] Water, Energy and Environmental Laboratory (L3E)-National Engineers College of Sfax (Tunisia) (ENIS). Street of Soukra Km 3.5, BP.W: 3038 Sfax-Tunisia. E-mail address: nazouhmoka@gmail.com/ salem_bouri@yahoo.fr

[b] Geology and Environmental Laboratory, Institute of Earth Sciences, University of Setif, Algeria - E-mail address: slimdem@yahoo.fr/hadjirihab@yahoo.fr

[c] Faculty of Sciences of Gabes. Department of Earth Sciences. City Campus Erriadh-Zirig 6072 - Gabes-Tunisia - E-mail address: hamed_younes@yahoo.fr

[d] Scottish Universities, Environmental Research Centre, SUERC, Rankine Avenue , Scottish Enterprise, Technology Park , East Kilbride, Glasgow, G750QF, Scotland. UK

E-mail address:adrian.boyce@glasgow.ac.uk

[e] Department of Earth Sciences,University Badji Mokhtar 23000. Annaba -Algeria. E-mail address: rabahlaouar@yahoo.fr

[f] Water resources division of Gafsa-Tunisia. E-mail address: abedazizdre@yahoo.fr

ABSTRACT

The hydrodynamic of the multi-aquifer system (the Continental Intercalaire " C.I " and the Complex Terminal " C.T ") of the North Gafsa basin is largely determined by tectonics (Tebessa - Gafsa fault). The composition of groundwater is controlled by complex reactions at gas-liquid-solid "mineralogical composition of associated rocks" interfaces, which depend on the natural surrounding and potential anthropogenic impact. The hydrochemical data (major ion geochemistry) indicate that these groundwaters are characterized by the dominance a Ca-Mg-HCO_3/SO_4 and Na-Cl-NO_3 water types. Geochemical pattern is mainly controlled by the

dissolution of halite, gypsum and/or anhydrite as well as by the incongruent dissolution of carbonate minerals. The pH of these samples range from 6.54 to 8.89, supporting the conclusion that the H_2CO_3/HCO_3 couple control pH buffering. Oxygen-18 ($\delta^{18}O‰_{SMOW}$) and deuterium ($dD‰_{SMOW}$) isotopic data show the exchange between the groundwater and the rock (water-rock interaction) and the evaporation effect. The isotopic content of the boreholes waters is of mixed Mediterranean - Atlantic origin and is opposite to the quantity of rainwater distribution, both in space and time in the study area. This is due to its geographical situation in the southern and south-western of the Mediterranean Sea and between the Atlas area and the Sahara Platform. The concentrations of the isotopic composition of the groundwater are significantly higher than the rainwater. This is indicative of the dissolution of salts and other processes modifying the rainwater geochemical composition during infiltration into the vadose zone. The hydraulic interconnection of these components of the system has led to the evolution of these interesting groundwater types.

Keywords: Groundwater, Multi-aquifer system, Dissolution, Isotopic composition, Tunisia.

1. Introduction

In the North African basin, water harvesting played a crucial role in ancient civilisations such as the Roman. During the 20^{th} century, modern techniques (groundwater drilling, “Foggara/Mkayel”, large reservoir construction “Majel and/or Fiskhiya” etc.), which are favoured by government policy, slowly replaced traditional harvesting techniques. High demands for water during the industrial period and agricultural growing season, which coincides with the dry period of the Mediterranean climate, has resulted in the deterioration of the water and in the depletion of the piezometric water table in many regions of the North Africa and especially in Tunisia. The scarcity of water resources in semi-arid sedimentary basins, the low renewal rate of groundwater resources and the poor water quality in the

Mediterranean basin make it necessary to find other water supplies and to revive traditional systems of water harvesting. Continuously increasing abstraction of groundwater resources to meet rising industrial, agricultural, domestic and touristic needs, coupled with severe drought periods during the past decades leads to growing deficit of water.

Due to different hydrogen and oxygen isotopic compositions of different water sources, stable hydrogen and oxygen isotopic ratios (δD and $\delta^{18}O$) are an excellent way to fingerprint the route of groundwater recharge and discharge (Craig, 1961; Clarke and Fritz, 1997). Tritium isotope (T) is always introduced into the hydrological circulation and dated with the fallout from atmospheric nuclear weapon tests conducted mainly during the early 1960s. It can be indirectly used to evaluate the rate of groundwater circulation and renewal rate (Clarke and Fritz, 1997). The application of isotope-based methods has become well established for water-resource assessment, development and management in the hydrological sciences, and is now an integral part of many water quality and environmental studies (Clark and Fritz, 1997; Cook and Herczeg, 2000). Environmental isotope techniques, hydrogeochemical analysis and hydraulic data are employed to identify the main recharge areas, the hydrodynamic, the mineralization of the hydrogeological basin and the impact of climate change on groundwater in the study area, one of the most important aquifers of central Tunisia. The utilization of these methods is the goals of the present paper.

2. Site description

North Africa and the southern Mediterranean basin during the Cretaceous that has held sway since the discovery of the salinity Crisis (Swezey, 2003) has been dominated by varying degrees of aridity (≈1000 m of evaporates in Tataouine basin and ≈250m in Maknassy and in Thelja basins) and humidity (Continental Intercalaire groundwater in North Africa area) during the Cretaceous period (Hamed et al., 2012a,b, 2013b). These factors are surely

indicators of dry and humid climates in North Africa. This is natural enough given the magnitude of the drying and warming of the Mediterranean Sea itself (Kallel et al., 1997a, 2000; Jedoui et al., 2001; Boussetta et al., 2012).

The study area is characterized by hilly topography and flat plateau surfaces with average elevation of 800 m a.s.l. The central of Tunisia is characterized by the absence of high mountains and a relatively limited geographic extension, allowing the integration of Saharan Platform air streams into the atmospheric circulation (Celle-Jeanton et al., 2001a). However, due to its position in the western and in the southern of the Mediterranean Sea, it represents a climatic transition zone open to desert and monsoon system (Kallel et al., 1997a, 2000; Jedoui et al., 2001; Zouari et al., 2003; Hamed, 2004; Kamel, 2007; Abidi, 2007; Essalami et al., 2007; Dassi, 2009; Ben Moussa et al., 2010a,b; Rouis-Zargouni et al., 2010; Hamed et al., 2012a; Mokadem et al., 2014). Indeed, regional hydro-meteorological studies (Celle, 2000; Celle-Jeanton et al., 2001b) mention the existence of two major trajectories for dominant air masses (Fig. 1A). These are : (i) the North Atlantic warm air masses that circulate from the west over the Northern Africa and (ii) the Mediterranean cool air masses that derive from the north. The study area, which is located in central Tunisia, covers an area of 3750 km^2 and lies between the longitudes 7º30'- 9°00'E and the latitudes 33°00'- 34º30'N (Fig. 1B). It corresponds to a synclinal structure limited in the South by the Gafsa Mountains (J.Bouramli, J.Ben Younes and J.Orbata), in the north by the Monts of Sidi Aïch and Souinia, in the west by Algerian territory and in the east by the Gabes Gulf (Fig. 1B). The North Gafsa basin is located approximately 100 km east of the Atlas Monts of North Africa. Elevations decrease from 2000 m above mean sea level in the west (Algerian Atlas: recharge area) to 500 m in the east (Aguila-El Jar plain: discharge area). In the study area, the spatial distribution of precipitation is strongly influenced by the relief.

The study area has undergone an arid to semi-arid climate changes marked by seasonal contrasting climatic variables. Influenced by a temperate Mediterranean climate, with moderately hot summers and cold winters. Rainfall gradually decreases from the Atlas range (North) to the Sahara Platform (South). It shows a mean annual rainfall of about 350 mm.year^{-1} (data based on observations from 1964 to 2013, Yermani et al., 2002; Mokadem et al., 2012, 2014) with a maximum amount of rainfall from November to February. The maximum rainfall amounts are associated with the highest elevations (J.Orbata ≈ 1100 m) of the study area (Fig. 1B). Mokadem et al. (2012) estimated an average annual precipitation of about 150–250 mm.year^{-1} and a potential evapo-transpiration of about 1680 mm.year^{-1} (Yermani et al., 2002; Mokadem et al., 2012, 2014). The mean annual temperature is 25°C; in January (winter) temperature is about 10°C. In July (summer) temperature ranges between 35 and 45°C (data from 1984 to 2013). The drainage net is composed of the Al Kebir, Sidi Aïch, El Maleh and Bayeich non-perennial wadis which collect surface runoff from the surrounding hills of Gafsa, Sidi Aïch, Souinia ranges and especially from the Algerian territories (Bir El Ater and Tebessa basins). The surface water of these wadis is carried to the large continental depression of Chott Djerid, south of the Gafsa basin (Fig. 1B).

3. Geology and Hydrogeology

Depositional facies of the aquifer sediments in the study area change from west to east and from north to south, from alluvium in the west and the north to marine sediments on the Gafsa plain (piedmont area). In the North Gafsa basin, the hydrogeology is largely controlled by tectonics. This basin has been affected by both compressional and extensional fault networks during the Mesozoic (Bédir et al., 2001; Zouaghi et al., 2009, 2011), which created several multi-layered framework (Coque, 1962; Boltenhagen, 1985a; Zargouni, 1985; Soyer and Tricart, 1987; Zouari et al., 1990; Outtani et al., 1995; Bouaziz et al., 2002; Feki et al.,

2005a,b; Ahmadi et al., 2006, 2013; Hamed, 2011; Mokadem et al., 2014). This basin is covered by Mio-Plio-Quaternary sediments which may reach 500 m in thickness according to drilling data and geophysical studies (Zouaghi et al., 2011) lying on sedimentary relicts from Cretaceous and Tertiary periods. The hydrostratigraphic units in the North Gafsa region are shown in Figure 2. The lithologic units in the study area extend from the Trias to the Quaternary. The Cretaceous series, which outcrops in the surrounding Mountains of the study area, constituted mainly of fractured/karstified carbonates, clay and sandstone deposits (Zargouni, 1985; Outtani et al., 1995; Henchiri and S'Himi, 2006). The study area consists of three groundwater systems, the shallow and the unconfined Tertiary-Quaternary aquifer systems, which unconformably overlies the confined aquifers of C.I of North Africa. These units consist of three main aquifer systems, namely, from the bottom to the top, the Continental Intercalaire (C.I), the Complex Terminal (C.T) and the alluvial aquifer of Om al Gsab (western part of the study area). They are from the bottom to the top (Figs. 1 and 2):

(i)-The deepest aquifer, which is a confined reservoir in almost the entire of the study area, with the exception of Sidi Aïch region. The geological formations which host the C.I aquifer are composed by fluvio-deltaic continental deposits (Cornet, 1964; Castany, 1982; M'Rabet, 1987; OSS, 2003, 2008; Gallala et al., 2009) producing intercalations of detrial levels with horizons of clay silts and frequent gypsum layers. The C.I aquifer is located within a succession of clastic sediment of Mesozoic age, the thickness and lithology of which vary laterally (UNESCO, 1972; M'Rabet, 1987). The groundwater of the C.I is mainly paleo-groundwater (30-35Ky) which dates back to the Pleistocene and early Holocene under a cooler and humid climatic regime (UNESCO, 1972; Edmunds et al., 1997; OSS, 2003, 2008). The water resource potential of this confined aquifer is not completely exploited due to its relatively great depth and the moderate quality of its groundwater. Hence, it is tapped only by a limited number of public wells in the Sidi Aïch basin with flow rates varying between 2 and

4 l/s (DGRE, 2010). It is also drained by several geothermic springs in the Ben Younes Mont in the south of the study area with a flow varying between 0.5 and 2 l/s (Yermani, 2000; Bouri, 2008; Bouri et al., 2008; Hamed et al., 2013d). The C.I has its recharge source in the Algerian and Tunisian Atlas Mountains (Appelgren, 2002). It is mainly confined and discharges in the Chotts Djerid (10,000 Km^2) of Tunisia, in the Chott Melhir of Algeria continental depressions and in the Gabes Gulf (Mediterranean Sea, Fig. 1A) (Ben Dhia, 1987; Swezey, 2003; Guendouz et al., 2003; OSS, 2003; Hamed et al., 2010b; Kamel, 2012; Hamed et al., 2013a). Recent recharge is observed at the periphery of the Sahara basin (Edmunds et al., 1997). In the North Gafsa region, the continental formations extend from the Neocomian at the base to the Albian. In the Lower Cretaceous only "Boudinar" and "Sidi Aïch" Formations constitute the productive levels of the C.I aquifer in the study area. Increasing water extraction has resulted in a decrease in the groundwater pressure in many places in this mining basin (OSS, 2003, 2008; Hamed et al., 2012b, 2013b; Hamed et Dhahri, 2013; Mokadem et al., 2014).

(ii)- The intermediate aquifer, which is semi-confined unit of C.T. It covers the major part of central and South Tunisia and the northern Sahara of North Africa (Algeria, Tunisia and Libya) (≈250,000 Km^2, UNESCO, 1972; OSS, 2003, 2008). The term Complex Terminal describes a multi-layer aquifer which consists of the Upper Cretaceous formations in the northern Saharan basin, i.e. the Upper and Lower Senonian and sandy formations of the Eocene and the Mio-Pliocene. The C.T formations are relatively heterogeneous and are composed of three main aquifer horizons separated by semi-permeable to impermeable strata (aquitard). The main productive levels are located either in the carbonates levels of the Upper Cenomanian Zebbag Formation (thickness varying between 300 and 600 m) and Upper Senonian Abiod Formation (100 <thickness<500 m) in the study area (Yermani, 2000;

Hamed, 2011; Hamed et al., 2012a,b,c; Mokadem et al., 2013a,b). The Upper Cretaceous is formed by a flag white fissured and kastified limestone and mainly drained through several springs near or in the ranges with a flow varying between 0.5 and 5 l/s. This fluctuation varies with several factors such as climatic and anthropogenic activities (Yermani, 2000; Hamed, 2011; Mokadem et al., 2014).

Concerning the Miocene aquifer (Beglia Formation): it is constituted by coarse sand interbedded by red clays and quartz, which indicate clearly a humid paleoclimate and a paleogeography dominated by perennial fluvial system with SW-NE paleo-drainage network direction (M'Rabet, 1987; Souayed, 1995; Gallala et al., 2009; Hamed et al., 2013b). The thickness of sand ranges from 50 to 400 m, the maximum thickness is observed in the southern of the study. To the top, we find the Pliocene-Quaternary aquifer (Segui Formation) is considered as the footwall of Quaternary sequence and has been reached by several private boreholes. Quaternary formation is much thicker than 200 m at north-western part of the basin (Sidi Boubaker region: Al Azaeiz borehole) and formed by alternation and interbedded by sands and clays (Hamed, 2011; Hamed et al., 2013b; Mokadem et al., 2014).

(iii)- The shallowest aquifer, which is exploited especially in irrigation use in Sidi Aïch plain and Om al Gsab basin in the west of the study area. This unconfined shallow aquifer is essentially recharged by the excess of irrigation water coming from C.T deep aquifers, in irrigated area (irrigation channels/sub-surface dams) and recharged during the rainfall events. Because of its high permeability, it contains a good quality of its groundwater.

The deposition of these sediments was followed by the flood plain and then the aeolian deposition of the sands. Within the study region, the total thickness of the unconfined aquifers ranges from approximately 100 m in the northeast and decreases south toward the basin margin (Fig. 2). Evaporites are abundant in the Quaternary deposits, and are dominated by halite and gypsum. These evaporitic sediments are present as a salt crust at the surface and

sub-surface. The halite has also been found in cores from the lake bed (Garâat Sidi Aïch in North part and Chott El Guettar, Garâat Douza and Sebkhat El Maleh in the South part of Gafsa basin) (Hamed, 2009a, 2011; Mokadem et al., 2014).

The flow direction of the groundwater of these aquifers is generally towards the Chott Djerid depression, (N-S, NW-SE and NE-SW) from a high in the potentiometric surfaces in Gafsa Monts toward the low potentiometric surfaces in Gafsa city (Yermani, 2000; Hamed, 2011; Mokadem et al., 2013a,b, 2014). Divergent flow directions were observed from the surface water network, highlighting the significant role of the aquifer recharge from the wadies. The cones of depression have become the dominant influence on groundwater flow directions, resulting in hydraulic gradients directed from the NW and NE freshwater areas towards the southern saltwater (overexploitation and residence time effects). The groundwater flow varies in space and time and is dependent on the climate effect, the properties of the rocks (texture and structure), the boundary conditions and the intercommunication with the hydrological and hydrogeological system. Topography and the differences in geology (i.e. differences in hydraulic conductivities) mainly determine the rate and direction of groundwater and surface water flow (Fig. 2). The configuration of the land surface of the study area is responsible for the variation in groundwater chemistry and the isotopic signature of the groundwater. Hydrogeologically, the seismic activity has played a major role in the hydrodynamic functioning of these aquifers and of their intercommunication (Zargouni, 1985; Ben Ayed, 1986; Boukadi et al., 1991; Dlala and Hfaiedh, 1993; Addoum, 1995; Outtani et al., 1995; Gouasmia, 2008; Hamed, 2009a). The groundwater flow directions of these aquifers (C.I and C.T) follow generally the surface water flowing. In fact, they are discharged into Chott Djerid salt lakes (Mamou, 1990; Yermani, 2000; Hamed, 2011; Mokadem et al., 2014).

4. Materials and methods

From January to February 2013, 87 shallow, deep wells (using a submersible pump) at different aquifer depths (from both open wells and tube wells) and springs in the North Gafsa basin were sampled and the specific well data and the associated onsite hydrochemical parameters recorded (see sampling sites in Fig. 3). Specific well data included location description, global positioning system (GPS) co-ordinates, well type and construction type, pump type and service life (if any) and static groundwater level. Multi-parameter measuring equipment from WTW, type Multi 340 was used for the onsite analysis. These were equipped with appropriate measuring probes (all by WTW): pH, temperature, Specific electrical conductivity (EC) and total dissolved solids (TDS). The groundwater collected from wells is different in depth ranging from 10 to 510 m and comprise mostly active municipal wells. Sampling was carried out close to the well heads. Prior to sample collection, inactive wells had been pumped until constant conductivity was reached to ensure sampling of primary groundwater.

The concentration of the dissolved inorganic carbon species bicarbonate, carbon dioxide and carbonate were determined, where relevant, by onsite titration. The alkalinity of the water samples was determined from a 100-ml aliquot by titration with 0.1 N HCl to an end point of pH=4.3. The end point is determined using a pH measuring apparatus (WTW-Multi 340i) with a glass electrode. The dissolved CO_2 concentration is determined analogously by titration with 0.1 N NaOH to an endpoint of pH=8.2. After that, sample bottles were filled and kept in a refrigerator upon collection. The geochemical analysis (major and trace elements) were carried out in the Water Institute of Technology of Gabes (ISSEG)-Tunisia, using a Dionex DX 100 ion chromatograph equipped with a CS12 and an AS14A-SC Ion Pac columns and an AS-40 auto-sampler. The saturation with respect to same minerals and the partial pressure of carbon dioxide (pCO_2) of all sampled water were determined using the

WateqF subroutine program (Plummer et al., 1992). Samples revealing relatively high salinity (exceeding 3 $g.l^{-1}$) were diluted before analysis. The quality of water analyses was checked from cation–anion balance by the relative deviation from charge balance:

$$(\Delta_{meq} = 100 \cdot (\Sigma_{meq+} - \Sigma_{meq-})/(\Sigma_{meq+} + \Sigma_{meq-}) < 6\%).$$

A limited number of water samples (15 boreholes) were selected for isotope analysis (^{18}O and ^{2}H). The $^{18}O/^{16}O$ and D/H isotopic ratios (expressed as $\delta^{18}O$ and δD‰ V-SMOW) in water samples were performed in the laboratory of the Scottish Universities Environmental Research Centre, Glasgow, Scotland. UK. Oxygen isotopes were analyzed using the CO_2-H_2O equilibration method proposed by Epstein and Mayeda (1953), followed by analysis on a mass spectrometer. Hydrogen isotopic ratios were measured on H_2 after the reaction of 10 mL of water with metallic zinc at 500 °C (Coleman et al., 1982). Oxygen and hydrogen isotopes analyses were reported to δ notation relative to Vienna-Standard Mean Oceanic Water (VSMOW), where $\delta = [(R_S/R_{SMOW}) - 1] \times 1000$; R_S represents either the $^{18}O/^{16}O$ or the $^{2}H/^{1}H$ ratio of the sample, and RSMOW is $^{18}O/^{16}O$ or the $^{2}H/^{1}H$ ratio of the SMOW. Typical precisions are ±0.1 and ±1.0% for oxygen-18 and deuterium, respectively. Oxygen-18 and deuterium groundwater samples were collected in glass phials. These phials were rinsed using the groundwater sample and were later filled in the flow cell and sealed beneath the water surface using an air-tight plastic lid. The stable isotope analysis using a mass spectrometer.

5. Results and discussion

5.1. *In situ* measurements interpretation

The results of geochemical analysis, *in situ* parameters such as pH, temperature, electric conductivity (EC) and total dissolved solids (TDS) together with analytical data of the major ions in groundwater samples are shown in Table 1. The pCO_2 in the groundwater

ranging between 0.15 10^{-3} and 36 10^{-3} atm compared to the precipitation pCO_2 of $10^{-3.5}$ atm suggested that the water gained CO_2 from root respiration and the decay of soil organic matter. Subsequently, an increase in pCO_2 caused a drop in pH (Fig. 4). The groundwater pH values range from 6.54 to 8.89 and the temperature varies within a wide range of 17 - 29.1°C, indicating the combination effects of numerous factors, i.e. the depth to groundwater, the residence time in the flow system and/or the groundwater flow time from the recharge area. This pH buffering reflects interaction between the H_2CO_3/HCO_3 couple and results from the hydration of CO_2 gas in water to form H_2CO_3 and later dissociation of H_2CO_3 to form HCO_3 and H^+. The EC and the TDS range from 0.2 to 9.96 $mS.cm^{-1}$ and from 0.1 to 14 $g.l^{-1}$, respectively (these parameters range from fresh to brackish water). Groundwater salinity in the study area varies both in the vertical and lateral directions. Higher values of these parameters characterize wells located in the central and the southern parts of the basin especially in the Swaï area and Aguila-El Jar oases suggesting the anthropogenic activities (agricultural and industrial). Generally, TDS (0.1 - 14 $g.l^{-1}$) increases from the mountainous regions (the piedmont zone of the Gafsa chain in the North of the study area, which characterize the recharge areas) towards the discharge area (southern part), as a result of the scarcity of recharge in these regions, the relatively long-term water–rock interaction. But, unexpected high salinities were measured in the Sidi Ahmed Zaroug area (overexploitation by CPG/GCT de M'Dhilla) and North Gafsa plain: Swaï area (North parts of the basin: irrigated basin) (Fig. 5). These high salinities are not in agreement with the general evolution of the mineralization in the direction of the surface water and the groundwater flow direction (N-S). This situation is explained specially by the impact of the application of nitrogen fertilisers. Others reasons for the elevated of the EC and the TDS in groundwater could include: percolation of sewage with high salt concentrations from drainage pits into the shallow groundwater; upwelling/inrush of deep groundwater of C.I, the contact geothermal

groundwater-evaporate Triassic sediments; relative enrichment of salts during groundwater recharge with a highest evaporation; anthropogenic (agricultural and industrial effects) via infiltration from the recent and the fossil drainage network.

Strong correlations exist among the major elements, Na, Ca, Mg, SO_4, NO_3 and Cl versus TDS (Fig. 6). These relationships clearly identify the main elements contributing to the groundwater salinity and their tendency to follow a similar trend (due to concentration by evaporation, dissolution and human activities). But there are moderate correlations between HCO_3 and K with TDS indicates that these ions tend to increase in concentration as the salinity of the water increases. The concentrations of potassium are low; it is due to the high consumption by the photosynthetic plants. The salinization of the groundwater would be expected to result from the ionic concentrations increasing due to both evaporation of recharge water and to the effects of interactions between the groundwater and the geological formations (Triassic deposits to alluvial sediments).

5.2. Major element geochemistry

Water types

Water types were defined by use of the trilinear plotting technique (Piper, 1944; Ophori and Toth, 1988; Kirchner, 1994); the trilinear diagrams are shown in figure 7. Based on the contents of major cations (Ca^{2+}, Mg^{2+}, Na^{+} and K^{+}) and anions (Cl^{-}, HCO_3^{-}, NO_3^{-} and SO_4^{2-}) (Table 1), two hydrochemical facies could be identified including facies (i)- Ca–Mg–HCO_3/SO_4 (predominant water type in the carbonate-rock aquifers because calcite, dolomite and silicates are abundant in these aquifers) and facies (ii)- Na–Cl–NO_3.

The majority of the water sampled are saturated/under-satureted with respect to calcite ($CaCO_3$) and dolomite $CaMg(CO_3)_2$ ($-0.88 \leq SI_{(calcite)} \leq 1.27$, $-1.93 \leq SI_{(dolomite)} \leq 2.3$ and $-1.03 \leq SI_{(aragonite)} \leq 1.07$). This stage indicates saturation (or equilibrium) or near saturation with respect to these carbonate minerals. Carbonate dissolution may occur systematically for the majority of groundwater samples. For groundwater samples, there is an under-saturation state with halite ($-7.6 \leq SI_{halite} \leq -4.65$), gypsum and anhydrite ($-1.51 \leq SI \leq 0.97$) (Table 2), indicating possible dissolution of these minerals. These eventual dissolutions were confirmed by strong positive relationships of Na versus Cl and Ca versus SO_4 (Figs. 8a,b) as well as by the positive correlations between the SI of the referred dissolved minerals and some of ions resulting from each dissolution (Figs. 9a,b). The plot of Na vs Cl can be used as a first order indicator of water-rock interaction. Although Na^+ and Cl^- exhibit a good correlation (Fig. 8a), halite dissolution may exert a control on the Na^+ and Cl^- chemistry. The Ca versus SO_4 binary relationship shows that most groundwater samples indicating obvious excess sulfate (Fig. 8b). This depletion of Ca can be attributed to the exchange, occurring between groundwater and clay minerals (Ca-Na cation exchange), which are relatively abundant in the MPQ strata (Chaabani, 1995; Ounis et al., 2006; Felhi et al., 2008; Felhi, 2010; Aloui et al., 2012). However, reverse cation-exchange process is confirmed through the plot of (Na+K–Cl) versus [(Ca+Mg) – (HCO_3+SO_4)], in which the two members vary in inverse proportions (Fig. 10) (Mc Lean et al., 2000; Garcia et al., 2001; Mokadem et al., 2012, 2014). The other possibility of this excess of sulfate is the anthropogenic activities indicative of pollution through land use practices due to the presence of the biochemically related elements SO_4, P, NO_3 and K, which are principal plant nutrients in the North Gafsa basin (Hamed et al., 2013c). The geochemical and hydrologic processes responsible for the various water types in the study area are discussed in the following sections:

(i)- Ca–Mg–HCO_3/SO_4 water type: this water type is predominant in the great part of the recharge areas (generally Quaternary alluvial deposits and at the topographically higher areas formed by fractured carbonates and sandy deposits of the Cretaceous). They are a direct result of incoming rainfall (with a low pH) and the subsequent dissolution of carbonate minerals and weathering of silicate rocks (reactions 1, 2 and 3). Also, if silicate weathering is a probable source of sodium, the water samples would have HCO_3 as the most abundant anion (Rogers, 1989). This is because of the reaction of the silicate minerals with carbonic acid in the presence of water, which releases HCO_3 (Elango et al., 2003). HCO_3 is the dominant anion in groundwaters of this basin. The anaerobic degradation of organic matter and proton exchange can produce this composition in water (Ako et al., 2012). The predominance of this water type is in the carbonate-rock aquifers (Lower and Upper Cretaceous), is generally produced by dissolution of the carbonate minerals (calcite and dolomite). High calcium and magnesium concentrations make the groundwater "hard" or "very hard". This significant hardness gives the water a very high buffer capacity against acid input, which is useful, for instance, to buffer the formation of acid from the nitrification of ammonium. From a technical point of view, hardness is very undesirable due to the potential incrustation build-up in pipelines and household appliances. The significant hardness is of course associated with high carbonate hardness and bicarbonate concentrations. The reaction of these minerals with water and carbon dioxide can be written as follows:

$$CaCO_{3(calcite)}+H_2O+CO_{2(pedogenic\ gas)}<==>Ca^{2+}+2HCO_3^- \quad (1)$$

$$CaMg(CO_3)_{2(dolomite)}+2H_2O+2CO_{2(pedogenic\ gas)}<==>Ca^{2+}+Mg^{2+}+4HCO_3^- \quad (2)$$

The predominance of sulfate over bicarbonate and the lack of agreement of the Ca–Mg–SO_4 water with the simple dolomite dissolution model indicate that other processes are controlling the chemistry of this water type. Two reactions can produce this type of water: (1)

dedolomitization, which involves dissolution reactions with carbonate minerals and gypsum, and (2) sulfuric acid neutralization, which involves dissolution of carbonate minerals with sulfuric acid generated by the oxidation of pyrite which comes from the phosphate rock (Chaabani, 1995; Ounis et al., 2006; Felhi et al., 2008; Felhi, 2010; Aloui et al., 2012). Dissolution of dolomite causes increases in the concentration of magnesium in the water. The overall reaction can be written as:

$$CaMg(CO_3)_2(s)_{(dolomite)}+CaSO_4 \quad 2H_2O(s)_{(gypsum)}+H^+ \leftarrow == \rightarrow CaCO_3(s)_{(calcite)}+Ca^{2+}+Mg^{2+}+SO_4^{2-}+HCO_3^-+2H_2O \qquad (3)$$

(ii)- Na–Cl–NO_3 water type: this water type predominates in the discharge zones (Aguila-El Jar area) reflects the dominance of sodium and chloride; and the influence of agricultural activities where flood irrigation is applied in the study area. However, this water type is rare in other parts of the carbonate-rock aquifer. Research C.I and C.T aquifers in this study area (Hamed, 2011) indicates two potential sources of sodium, chloride and nitrate to these aquifers. In the discharge zones, shallow groundwater (MPQ) in highly permeable outwash valleys contains elevated concentrations of this facies that are related to human activities "influence of the excessive use of $Ca(NO_3)_2$ fertilizers (300-600 $kg.ha^{-1}.year^{-1}$)" (Hamed et al., 2013b; Mokadem et al., 2014).

Nitrate geochemistry (Land use)

Nitrogen fertilizers are applied extensively in agriculture to increase crop production, but excess nitrogen supplies can cause air, soil, and water pollution (Wick et al., 2012). Nitrate pollution of water is of high concern as it may have negative impacts on water supply and ecosystems (Rouabhia et al., 2004, 2008a; Hamed, 2009a; Ben Moussa et al., 2010a; Darwish et al., 2011; Diédhiou, 2012; Hamed et al., 2013a). Nitrate (NO_3^-) is a familiar pollutant in groundwater. Large amounts of nitrate in drinking water are a cause of

methemoglobinemia (blue baby syndrome), a blood disorder primarily affecting infants under 6 months of age (Bengtsm and Annadotter, 1989; Avery, 1999), cancer through the formation of carcinogenic N-nitroso compounds (Weyer et al., 2001), to spontaneous abortions (Centers for Disease Control and Prevention, 1996), and to non-Hodgkin's lymphoma (Ward et al., 1996). As nitrate contamination is related to human, animal, or industrial waste practices, excessive levels of nitrate in drinking water may indicate the presence of other types of contaminants, which may cause health problems. Therefore, nitrate concentration is an important criterion of groundwater quality. Furthermore, nitrate is one of the important parameters that can be traced easily and used for assessment of contamination risks due to its low degree of attenuation of the contaminant load in the soil matrix and water. In the North Gafsa basin unconfined aquifer, the nitrate concentrations vary within a large range from 0.4 to 91.44 mg/l. About 16.1 % of samples have nitrate concentration that exceeds the drinking water standards of 38 mg/l (25-50 mg/l) (WHO, 2006). The average value of nitrate in the whole groundwater samples is 45.92 mg/l. These high nitrate concentrations provide evidence for the significance of the return flow irrigation waters contribution in the recharge of the unconfined aquifer. Mokadem et al. (2014), found that nitrate concentrations in groundwater were highest in areas where wastewaters were present in Gafsa oasis and in Swaï agricultural basin (Fig. 11). The high concentration of NO_3 ions in groundwater is indicative of the unconfined nature of the system and this also suggests that the groundwaters are very young in age. Indeed, ammonium nitrate, liquid fertilizer and other commercial complex nitrogen fertilizers are used in large scale in the agricultural regions to enhance productivity due to rapid population increase and development of technology, where flood irrigation is applied (Hamed et al., 2013a). In Gafsa basin nitrate occurs naturally in groundwater. However, septic leakage, nitrogen fertilizers, animal manure applied to soil and gases of the atmospheric pollution “industrial sector of M’Dilla-CPG/GCT-Gafsa” can cause elevated levels of nitrate

in groundwater. In these regions, NO_3 contents are up to 38 mg/l (Fig. 11). The excessive use of $Ca(NO_3)_2$ fertilizers is verified through the well-defined relationship between NO_3^- and Ca^{2+} (Fig. 12a). Similarly, the well-defined relationships in the plots of NO_3 versus SO_4 and Mg versus SO_4 (Figs. 12b,c) suggest that N and S are used in the study area in the form of $(NH_4)2SO_4$, $MgSO_4$ and superphosphate fertilizers, pesticides (atrazine "$C_8H_{14}ClN_5$", deethylatrazine, simazine, metolachlor, and prometon were detected more frequently in the study area) (Hamed et al., 2012b,c).

5.3. Isotopic study of groundwater pathways

Interpretation of oxygen-18 and deuterium data

Oxygen and hydrogen isotope compositions for the investigated CT groundwater samples are represented in the conventional $\delta^2H/\delta^{18}O$ diagram together (Fig. 13), with the Global Meteoric Water Line (GMWL) (Craig, 1961; Rozanski et al., 1993), the Local Meteoric Water Line (LMWL) of the Sfax city (Maliki, 2000; Celle et al., 2001) located at about 150 km from the study area, and the socalled ''Palaeo-Meteoric'' Water Line (PMWL) (Sonntag et al., 1978).

(i)- Craig (1961): $\delta^2H = 8\ \delta^{18}O + 10$ (Global Meteoric Water Line);

(ii)- Rozanski et al. (1993): $\delta^2H = 8\ \delta^{18}O + 10.8$;

(iii)- Maliki (2000) and Celle et al. (2001): $\delta^2H = 8\ \delta^{18}O +13.5)$ (LMWL).

The Global Meteoric Water Line (GMWL) corresponds to the averaging of numerous local meteoric straight lines, each of which is influenced by the abovementioned geographic and climatic factors (Rozanski et al., 1993; Andreo et al., 2004). The intercept of the GMWL is termed the deuterium excess (d-excess= δ^2H-8 $\delta^{18}O$ after Dansgaard, 1964). The value of this parameter is acquired during evaporation, and does not vary significantly during the later history of the cloud mass. It is thus a valuable indicator of the source area of the water vapor

(Rindsberger et al., 1983; Cruz Sanjulià n et al., 1992; Celle-Jeanton et al., 2001): d-excess values close to 10% indicate waters of Atlantic origin, values close to 22% are characteristic of waters from the Eastern Mediterranean and d values close to 14%, intermediate between the first 2, are detected in rainwater falling on the Western Mediterranean. This is thought to be due to particular climatic and environmental conditions which cause the instability of the air over the Atlantic Ocean and the Mediterranean Sea and consequently produce an intense exchange between moisture and the sea surface (Grassa et al., 2006-modified). Data from the nearest Global Network for Isotopes in Precipitation (GNIP) station number 7622500, located at Sfax city, were used to establish the Local Meteoric Water Line, that follows the linear regression and the Regional Precipitation Mean Value for $d^{18}O_{(VSMOW)}$ and $d^{2}H_{(VSMOW)}$ (-4.59 and -23.30%, respectively) (IAEA/WMO, 1999).

As suggested by Craig (1961), the slope of the $\delta D/\delta^{18}O$ line close to 8 suggests that precipitation takes place under near-equilibrium conditions, while lower values indicate the presence of kinetic fractionations. The isotopic composition of $\delta^{18}O$ and $\delta^{2}H$ values of all groundwaters in the study area ranges from -7.1‰ to -4.9‰, and from -60‰ to -37‰ respectively (Table 1). In the conventional $\delta^{18}O$ vs. $\delta^{2}H$ diagram (Fig. 13), most of the samples plot near the global meteoric line, suggesting that the groundwater is of meteoric origin (Craig, 1961). One sample plots to the left of the GMWL, showing about 1‰ enrichment in $\delta^{18}O$. This sample is the most diluted groundwater, and mixing probably influences its isotopic composition (meteoric contamination non evaporate). This evidence confirms, as expected, that the alluvial groundwater of north Gafsa basin originated from present rainwater. Furthermore, it indicates that rainwater has not undergone isotopic fractionation through evaporation before recharge (Gat and Gonfiantini, 1981). The localization of this sample confirms that these aquifers have been recharged by rainfall

derived from a mixture of Oceanic and Mediterranean vapor masses (Fig. 1A). These values of local precipitation are much higher than those supposed to be for the LC and UC groundwaters, indicating either a recharge altitude effect and/or a palaeoclimatic impact: recharge under humid and colder climatic conditions than at present day. This hypothesis of ancient recharge agrees with the results of Fontes et al. (1983), Ouda (2000), Yermani et al. (2002); Zouari et al. (2003) and Hamed et al. (2008 and 2010a,b) obtained in south Tunisia, which were interpreted as recharge occurring during the Late Pleistocene and the Early Holocene periods. This period Pleistocene and Holocene that could be responsible for the periodic recharge of old groundwaters in the North Africa. In the last 70 ka before present (MIS 2 and MIS 3,Würm period), three major humid phases have been identified: (i)- the Early Würm pluvial (MIS 3), lasting from 70 to 40 ka before present, (ii)- the Middle Würm pluvial (MIS 3), from about 32 to about 22 ka before present and (iii)- the Late Würm pluvial (MIS 2), lasting from about 18 to 11 ka before present (Zuppi and Sacchi, 2004).

Although, the isotopic composition of all sampled solutions indicates the meteoric origin, their isotope signatures can be modified by evaporation of rain in the atmosphere and/or in the soil during infiltration as indicated by isotope values plotting below the meteoric water line (Clark and Fritz, 1997). The $\delta^{2}H$ and $\delta^{18}O$ values for the analysed surface waters plot below the LMWL and GMWL (see evaporation domain in Fig. 13). Evaporation results in discrimination of ^{18}O and ^{2}H versus ^{16}O and H, respectively, and heavier isotopes are accumulated in the remaining solution. If rainwater is infiltrated slowly into the ground, significant evaporation may take place prior infiltration (e.g. Allison, 1982; Hamed et al., 2008, 2010b). The homogeneity of the isotopic composition of large aquifers may reflect either very stable recharge conditions in time or very long residence time of water during which diffusion processes occured and smoothed any past fluctuations, as is the case in the

great regional North African aquifer "Continental Intercalaire" (Gonfiantini et al., 1974; Hamed et al., 2012a,b). In North Africa Sahara, the largest groundwater aquifer systems in the world of the C.I experienced a period of intense palaeorecharge (Humid phases and/or pluvial) from about 45-23.5 ky (interglacial periods in the Mediterranean basin) (Guendouz et al., 1997; Zuppi et Saachi, 2004).

In addition to evaporation, mineral dissolution and/or transpiration are important factors controlling the salinity of water bodies in arid areas. Because deuterium excess (Dansgaard, 1964) decreases during evaporation and is unrelated to the isotopic composition of the initial water, it can be used to assess the effect of evaporation. Dansgaard (1964) proposed the use of “d-excess” to describe the deuterium excess for global precipitation. The value “d” is defined for a slope of 8 and is calculated for any water sample as: d-excess=δ^2H - 8 $\delta^{18}O$. Globally, “d” averages 10‰ for precipitation. When a water body undergoes evaporation, the deuterium excess will decrease and the salinity will increase with a negative correlation. In North Gafsa basin during 2014, the average of “d-excess” is -1.9‰. The “d” values, varying from -14.4‰ to 10.6‰ (Table 1).

Assuming that chloride (Cl) in rainwater is entirely derived from marine aerosols, the content of Cl can be used to trace the origin of air masses and to follow their trajectories on land. Generally, concentrations of Cl^-, δD, and $\delta^{18}O$ values of groundwater have a positive correlation, which was considered as an index of waters from a deep, confined, and unconfined aquifer. Positive correlation of high EC and heavy $\delta^{18}O$ represents an evaporation effect on the water (during diffuse recharge, or due to groundwater discharge via evaporation). There are no obvious correlations between temperature and δD, $\delta^{18}O$ values and EC, or Cl^- values in the groundwater of the research area. These all indicate that surface cold water recharging the groundwater system has an important effect on groundwaters with slight

effect of evaporation. The dissolution of evaporates (halite, anhydrite and gypsum) and evaporation process are observed in the diagram of $\delta^{18}O$ vs. Cl (Fig. 14), which includes data for groundwater collected in the North Gafsa basin. The heterogeneity arrangement of the boreholes is mainly due to the dissolution of evaporate deposits. It is noted for about 40% of the groundwater samples that high chloride concentrations are not clearly correlated with the oxygen-18 contents. Nevertheless, about 60% of the samples show a good correlation between chloride and oxygen-18. For these samples, evaporation appears to be an important process, especially, for groundwater sampled in Swaï area (north Gafsa plain) where flood irrigation is particularly used. The extent of evaporation is expected to be variable with time mainly depending on climatic parameters (air temperature and humidity) as well as on the main features of rainy events (duration, intensity of the rainfall) precipitation originating from moisture coming from different regions or to exchange processes between moisture and large surfaces of water (e.g. seas and lakes) (Gat and Carmi., 1970; Sonntag et al., 1978; Hoffmann et al., 2000).

The principal areas of recent recharge (contamination by the meteoric fresh water) are located in: (i) infiltration from wadies flood waters (drainage network: El Kebir, El Maleh, Bayeïch wadies), (ii) irrigation channels, (iii) sub-surface dams of Om al Gsab (western part of the study area) and (iv) in Gafsa Monts uplands (Tunisia) and the Algerian Atlas where the Senonian calcareous formations are outcropping. In dual porosity systems the relatively rapid infiltration of rainfall via pores/fractures/faults results in recent water intercepting the water table, which mixes with relatively older groundwater that has more slowly infiltrated via the primary porosity of the matrix. Groundwater salinity is intrinsically linked to evaporation during recharge and discharge processes.

6. Conclusions

The combination of hydrogeological, major elements geochemistry and stable ($\delta^{18}O$, $\delta^{2}H$ and d-excess) isotopes has provided a comprehensive understanding of the hydrodynamic functioning and the mineralization processes that underpin the large variations in chemical composition within the North Gafsa basin (central Tunisia).

Groundwater pumped from the multilayer aquifers is an important production factor in irrigated oases agriculture and in industrial of CPG-GCT in central Tunisia. Human activities in the basin played a key role in the hydrological change of study area. Besides precipitation in the basin decreased between 1950 and 2014 due to the climate effect, which was another factor that led to water resources deficit and the decrease of groundwater water level and the decrease of spring outflow or even disappearance of springs in the central Tunisia. The hydrochemical data from this study permit to classify the groundwaters into two dominant main water types: Ca-Mg- HCO_3/SO_4 and Na-Cl-NO_3 water types. Which are the result of the dissolution of evaporate sediments (water-rock interaction), cation exchange and over-fertilisation. In areas of intensive exploitation, the zoned pattern of salinities is disrupted, showing that the pumping is having a major impact on flow fields and salinity distributions. The distribution of the salinities with depth depends on hydrogeological conditions, lithologic nature of rocks, such as the presence of local paleo-channels and confining strata aquifer, as well as the over-exploitation of groundwater and the climate impact.

Based on the stable isotopes of water molecule, it was possible to identify various types of groundwater and mixing process in the system: (i) an old palaeoclimatic groundwater. This groundwater was likely recharged during the Late Pleistocene and Early Holocene periods under a cooler climatic regime; (ii) a relatively recent groundwater, that

indicates the presence or the influence of fresh groundwater derived from meteoric sources (less than 50 years) or possible contamination of a groundwater sample with modern atmospheric water vapor during sampling. This groundwater is interpreted as contemporaneous recharge at the high-altitude surrounding mountains; (iii) a mixing groundwater resulting from the dominant upward leakage from the deep C.I artesian geothermal water table. The recharge of these aquifers in central Tunisia generally occurs through three major mechanisms: (i) direct infiltration of rain and; (ii) lateral percolation from wadies/dams/channels; and (iii) upwelling/inrush from surrounding deeper aquifers. Further chemical and isotopic analyses from water samples collected during the catchment's flow period will allow a better understanding of the geochemical functioning of the watershed and will allow modelling of water-soil-rock interactions. The results of such a study could be extended to explain the catchment chemistry and hydrodynamics of similar infiltrating reservoirs. The distribution of rainfall, in space and time, therefore, is a significant factor which conditions the variations of the ^{18}O and ^{2}H contents of rainwater, and consequently of groundwater. Thus, these environmental tracers can be applied to groundwater investigation in mountainous karst aquifers, where orography and hydrogeology are very complicated (Algerian and Tunisian Atlas).

Acknowledgements

Many thanks are due to anonymous reviewers who greatly improved an early version of the manuscript. The authors should like also to thank sincerely the numerous people who helped me in the preparation of this paper. The following list is not exhaustive, but perhaps more than most, the people listed will know of my interest in Quaternary climate.

References

Abidi, B., 2007. Caratérisation hydrogéologique, géochimique et isotopique des systèmes aquifères du synclinal de Tamerza et de la plaine de Chott El Gharsa (Sud Ouest Tunisien). Thèse Doctorat Univ. de Sfax.

Addoum, B., 1995. L'Atlas Saharien Sud-oriental : Cinématique des plis-chevauchements et reconstitution du bassin du Sud-Est Constantinois (confins algéro-tunisiens). Thèse Doc. Ès Sci. Univ. Paris XI Orsay.

Ako, A.A., Jun, S., Takahiro, H., Kimpei, I., George, E.N., Wilson, Y.F., Gloria, E.T.E., Ntankouo, N.R., 2011. Evaluation of groundwater quality and its suitability for drinking, domestic, and agricultural uses in the Banana Plain (Mbanga, Njombe, Penja) of the Cameroon Volcanic Line. Journal of Environmental Geochemistry and Health. http://dx.doi.org/10.1007/s10653-010-9371-1.

Allison, G.B., 1982. The relationship between ^{18}O and deuterium in water and in sand columns undergoing evaporation. J Hydrol 76:1-25.

Ahmadi, R., Ouali, J., Mercier, E., Mansy, J. L., 2006. The geomorphologic responses to hinge migration in the fault-related folds in the Southern Tunisian Atlas. J. Struct. Geol. 28 721-728.

Ahmadi, R., Eric, M., Ouali, J., 2013. Growth-strata geometry in fault-propagation folds: a case study from the Gafsa basin, southern Tunisian Atlas. Swiss Journal of Geosciences, doi 10.1007/s00015-013-0122-z (in press).

Aloui, T., Dasgupta, P., Chaabani, F., 2012. Facies pattern of the Sidi Aïch Formation: Reconstruction of Barremian paleogeography of Central North Africa. Journal of African Earth Sciences 71-72.18-42.

Andreo, B., Linan, C., Carrasco, F., Jiménez de Cisneros, C., Caballero, F., Mudry. J., 2004. Influence of rainfall quantity on the isotopic composition (^{18}O and ^{2}H) of water in mountainous areas. Application for groundwater research in the Yunquera-Nieves karst aquifers (S Spain) Applied Geochemistry 19 (2004) 561-574.

Appelgren, B., 2002. Scope of the International Workshop on Transboundary Aquifers in the African Region, Proceedings of the International Workshop Tripoli, Libya, 2-4 June.

Avery, A., 1999. Infantile methemoglobinemia: re-examining the role of drinking water nitrates, children health review. Environmental Health Perspectives 107 (7), 583-586.

Ben Ayed, N., 1986. Évolution tectonique de l'avant-pays de la chaîne alpine de Tunisie du début du Mésozoïque à l'Actuel. Thèse d'État, université Paris-11.

Bengtsm,G., Annadotter, H., 1989. Nitrate reduction in a ground water microcosm determined by 15N gas chromatograph mass spectrometry. Applied and Environnement microbiology 55 (11) 2861-2870.

Ben Dhia, H., 1987. The geothermal gradient map of central Tunisia, comparison with structural, gravimetric and petroleum data. Tectonophysics 142, 99-109.

Ben Moussa, A., Bel Haj Salem, S., Zouari, K., Jlassi, F., 2010a. Hydrochemical and isotopic investigation of the groundwater composition of an alluvial aquifer, Cap Bon Peninsula, Tunisia Carbonates Evaporites.Earth Env Sci 25:161-176. doi:10.1007/s13146-010-0020-7

Ben Moussa, A., Bel Haj Salem, S., Zouari, K., Marc, V., Jlassi, F., 2010b. Investigation of groundwater mineralization in the Hammamet-Nabeul unconfined aquifer, north eastern Tunisia: geochemical and isotopic approach Environ Earth Sci, doi 10.1007/s12665-010 0616-1.

Bedir, M., Boukadi, N., Tlig, S., Ben Timzal, F., Zitouni, L., Alouani, R., Slimane, F., Bobier, C., Zargouni, F., 2001. Subsurface Mesozoic Basins in the Central Atlas of Tunisia,

tectonics, sequence deposit distribution and hydrocarbon potential. A.A.P.G. Bull. 85, 885-907.

Boltenhagen, C., 1985a. Paléogéographie du Crétacé moyen de la Tunisie centrale. In: 1er Cong. Natio. Sci. Terre, Tunis, Tunisia, pp. 97-114.

Bouaziz, S., Barrier, E., Soussi, M., Turki, M. M., Zouari, H., 2002 . Tectonic evolution of the northern African margin in Tunisia from paleostress data and sedimentary record. Tectonophysics, 357. p. 227-253.

Bouri, S., 2008. Les ressources en eaux thérmo-minérales en Tunisie: Connaissance du gisement, gestion et protection. HDR. Fac. Sc. de Sfax. 145p.

Bouri, B., Makni, J., Ben Dhia, H., 2008. A synthetic approach integrating surface and subsurface data for prospecting deep aquifers: the Southeast Tunisia. Environ Geol. doi: 10.1007/s00254-007-0928-y.

Boukadi, N., Zarai, N., Ben Ouezdou, H., Zargouni, F., Chaouachi, A., Lâatar, E.,1991. Carte géologique de la Tunisie, Feuille de Oum Laâraïs (N° 59). Echelle 1/100 000. Edt. Service géologique, ONM.

Boussetta, S., Kallel, N., Bassinot, F., Labeyrie, L., Duplessy, J.C,. Caillon, N., Dewilde, F., Rebaubier, H., 2012. Mg/Ca-paleothermometry in the western Mediterranean Sea on planktonic foraminifer species Globigerina bulloides: Constraints and implications. C. R. Geoscience 344. 267-276.

Centers for Disease Control and Prevention, 1996. Spontaneous abortions possibly related to ingestion of nitrate-contaminated well water-La Grange County, Indiana, 1991-1994. Morbidity and Mortality Weekly Report 45, 569-572.

Cornet, A., 1964. Introduction à l'hydrogéologie saharienne. Revue de Géographique, Physique et de Géologie Dynamique (Part 2) VI (1), 5-72.

Castany, G., 1982. Bassin sédimentaire du Sahara septentrional (Algérie-Tunisie) - Aquifères du Continental intercalaire et du Complexe Terminal. Bulletin Bureau Recherches Géologiques Minières (BRGM). Série 2. 3. 127-147.

Celle, H., 2000. Caractérisation des précipitations sur le pourtour de la Méditerranée occidentale. Thèse, Doctorat Es Sciences, Université d'Avignon et des pays de Vaucluse, France. pp. 222.

Celle, H., Zouari, K., Travi ,Y., Daoud, A., 2001. Caractérisation isotopique des pluies en Tunisie. Essai de typologie dans la région de Sfax. C.R. Acad. Sci. Paris 6. 625-631.

Celle-Jeanton, H., Travi, Y., Blavoux, B., 2001a. Isotopic typology of theprecipitation in the western Mediterranean region at three different time scales. Geophys Res Lett 28(7):1215-1218.

Celle-Jeanton, H., Zouari, K., Travi, Y., Daoud, A., 2001b. Caractérisation isotopique des pluies en Tunisie. Essai de typologie dans la région de Sfax. Comptes Rendues Academie des Sciences Paris 333, 625-631.

Chaabani, F., 1995. Dynamique de la partie orientale du bassin de Gafsa au Crétacé et au paléogène. Etude minéralogique et géochimique de la série phosphatée éocène - Tunisie méridionale- Doct. Es.Sc Géologiques. Fac. Tun.II. 428p.

Craig, H., 1961. Isotopic variation in meteoric waters, Science, 133,1702-1703.

Clark, ID., Fritz, P., 1997. Environmental isotopes in hydrogeology. Lewis Publishers, New York, p 328.

Coque, R., 1962. La Tunisie présaharienne. Etude géomorphologique. Thèse Lettres, Paris éd.A.Colin,476p.

Cook, P., Herczeg, A.L., 2000. Environmental Tracers in Subsurface Hydrology. Kluwer, New York .

Coleman, M.L., Shepherd, T.J., Durham, J.J., Rouse, J.E., Moore, G.R., 1982. Reduction of water with zinc for hydrogen isotope analysis. Anal Chem 54:993-995.

Cruz Sanjulian, J., Araguas, L., Rozanski, K., Cardenal, J., Hidalgo, M.C., Garcia Lopez, S., Martinez Garrido, J.C.,Moral, F., Olias, M., 1992. Sources of precipitation over South-Eastern Spain and groundwater recharge. An isotopic study. Tellus 44B, 226-236.

DGRE, 2010 and 2012. (Direction Générale des Ressources en Eau) Annuaire de l'exploitation des nappes de la Tunisie. DGRE, Tunis.

Dassi, L., 2009. Use of chloride mass balance and tritium data for estimation of groundwater recharge and renewal rate in an unconfined aquifer from North Africa: a case study from Tunisia. Environmental Earth Sciences. doi:10.1007/s12665-009-0223-1.

Dlala, M., Hfaiedh, M., 1993. Le seisme du 7 Novembre 1989 à Metlaoui (Tunisie Méridionale): une tectonique active en compression. C.R.Acad Sci 317:1297-1307.

Dansgaard, W., 1964. Stable isotopes in precipitation. Tellus 16, 436-468.

Darwish, T., Atallah, T., Francis, R., Saab, C., Jomaa, I., Shaaban, A., Sakka, H., Zdruli, P., 2011. Observations on soil and groundwater contamination with nitrate: A case study from Lebanon-East Mediterranean. Agricultural Water Management, Volume 99, Issue 1, November 2011, Pages 74-84.

Diédhiou, M., 2012. Tracing groundwater nitrate sources in the Dakar suburban area: an isotopic multi-tracer approach. Hydrological Processes. 26: 760-770.

Edmunds, W.M., Shand, P., Guendouz, A.H., Moula, A., Mamou, A., Zouari, K., 1997. Recharge characteristics and groundwater quality of the grand erg oriental basin. Technical report Wd/97/46R, Vienna.

Elango, L., Kannan, R., Senthil Kumar, M., 2003. Major ion chemistry and identification of hydrogeochemical processes of groundwater in a part of Kancheepuram district, Tamil Nadu, India. Journal of Environmental Geosciences 10 (4), 157-166.

Epstein, S., Mayeda, T.K., 1953. Variations of ^{18}O content of waters from natural sources. Geochimica et Cosmochimica Acta 4, 213-224.

Essallemi, L., Sicre, M.A., Kallel, N., Labeyrie, L., Siani, G., 2007. Hydrological changes in the Mediterranean Sea over the last 30,000 years. Geochemistry, Geophysics. Geosystems 8, 7, doi:10.1029/2007GC001587.

Feki, M., Rigane, A., Gourmelen, C., 2005a. Tectonique distensive fini-Aptienne au Jebel El Hamra de Kasserine (Tunisie centro-occidentale). Notes Serv. Géol., Tunisie 73, 77-89

Feki, M., Rigane, A., Gourmelen, C., Belguith, Y., 2005b. Aptian distensive Tectonics in South-Tethyan margin in Tunisia: example of Jebel El Hamra (central Tunisia). In: Actes, the First International Conference on the Geology of the Tethys, Cairo University, vol. II, pp. 429-437.

Felhi, M., Tlili, A., Montacer, M., 2008. Geochemistry, Petrography and Spectroscopy of Organic Matter of Clay-Associated Kerogen of Ypresian Series: Gafsa-Metlaoui Phosphatic Basin, Tunisia. Resource Geology, Volume 58, Number 4, December 2008, pp. 428-436 (9).

Felhi, M., 2010. Les niveaux intercalaires de la series yprésienne du bassin Gafsa Métlaoui : Apports de la minéralogie des argiles et de la géochimie de la matière organique résiduelle à la reconstitution paléoenvironnementale. Ph.D. thesis, University of Sfax. pp 170.

Fontes, J.C., Coque, R., Dever, L., Filly, A., Mamou, A. 1983. Paleohydrologie isotopique de l´wadi el Akarit (sud tunisien) au Pleistocene et à l'Holocene. Pal. 43, 41-61.

Gallala, W., Gaied, M.E., Montacer, M., 2009. Detrital mode, mineralogy and geochemistry of the Sidi Aïch Formation (Early Cretaceous) in central and southwestern Tunisia: Implications for provenance, tectonic setting and paleoenvironment. Journal of African Earth Sciences 53 (2009) 159-170.

Grassa, F., Favara, R., Valenza, M., 2006 (modified). Moisture source in the Hyblean Mountains region (south-eastern Sicily, Italy): Evidence from stable isotopes Signature. Applied Geochemistry 21 2082-2095.

Guendouz, A., Moulla, A.S., Edmunds,W.M., Shand, P., Poole, J., Zouari, K., Mamou, A., 1997. Palaeoclimatic information contained in groundwater of the Grand erg Oriental, north Africa. In: International Symposium on Isotope Techniques in the Study of Past and Current Environmental Changes in the Hydrosphere and the Atmosphere. IAEA, Vienna, pp. 555-571. 14-18 April- IAEA-SM-349.

Guendouz, A., Moulla, A.S., Edmunds, WM., Zouari, K., Shand, P., Mamou, A., 2003. Hydrogeochemical and isotopic evolution of water in the Complex Terminal aquifer in the Algerian Sahara. J. Hydrol 11: 483-495.

Gouasmia, M., 2008. Etude géophysique des potentialités hydrauliques au SW de la région de Gafsa. Thèse Doctorat de 3^{éme} cycle. Université de Tunis II. Tunis. p. 200.

Gonfiantini, R., Conard, G., Fontes, J.Ch., Sauzay, G., Payne, B.R., 1974. Etude isotopique de la nappe du Continental Intercalaire et ses relations avec les autres nappes du Sahara septentrional. In : Isotope Technique in groundwater, Hydrology, march 1974. Proceed. Symp., IAEA, Vienna, I, 227-241.

Gat, J.R., Carmi, H., 1970. Evolution of the isotopic composition of atmospheric waters in the Mediterranean Sea area. J. Geophys. Res. 75, 3039-3040.

Gat, J.R., 1981. In: Geonfiantini, R. (Eds.), Stable isotope hydrology – deuterium and oxygen – 18 in the water cycle. International Atomic Energy Agency Technical Reports Series 210, pp. 223-239.

Gat, J.R., Gonfiantini, R., 1981. The isotopes of hydrogen and oxygen in precipitation. In: Fritz, P., Fontes, J.C. (Eds.), Handbook of Environmental Isotope Geochemistry, vol. 1A. Elsevier, Amsterdam, pp. 21-47.

Garcia-R, M., López, M., I., Vicente,S., M., Lasanta–Martínez, T., Beguería, S., 2011. Mediterranean water resources in a global change scenario. Earth Science Reviews 105, 121-139.

Hamed, Y., 2004. Caractérisation hydrogéologique, hydrochimique et isotopique des eaux souterraines de la région du Kef (Nord Ouest Tunisien). Mémoire DEA. Faculté de Sciences de Sfax, 180p.

Hamed, Y., Dassi, L., Ahmadi, R., Ben Dhia, H., 2008. Geochemical and isotopic study of the multilayer aquifer system in the Moulares-Redayef basin, southern Tunisia. Hydrological Sciences–Journal–des Sciences Hydrologiques, 53(5) December 2008.

Hamed, Y., 2009a. Caractérisation hydrogéologique, hydrochimique et isotopique du système aquifère de Moularés-Tamerza. Ph.D. thesis, University of Sfax, pp 280.

Hamed, Y., Zairi, M., Ali, W., Ben Dhia, H., 2010a. Estimation of residence times and recharge area of groundwater in the Moulares mining basin by using carbon and oxygen isotopes (South Western Tunisia). J Environ Protect 1:466-474.

Hamed, Y., Dassi, L., Tarki, M., Ahmadi, R., Mehdi, K., Ben Dhia, H., 2010b. Groundwater origins and mixing pattern in the multilayer aquifer system of the Gafsa-south mining district: a chemical and isotopic approach. Environ Earth Sci 63:1355-1368.

Hamed, Y., 2011. The hydrogeochemical characterization of groundwater in Gafsa-Sidi Boubaker region (Southwestern Tunisia). Arabian Journal of Geosciences doi: 10.1007/s12517-011-0393-5.

Hamed, Y., Ahmadi, R., Hadji, R., Mokadem, N., Ben Dhia, H., Wassim, A., 2012a. Groundwater evolution of the Continental Intercalaire aquifer of Southern Tunisia and a part of Southern Algeria: use of geochemical and isotopic indicators. Desalination and Water Treatment Journal. doi: 10.1080/19443994.2013.806221.

Hamed, Y., Ahmadi, R., Hadji, R., Mokadem, N., Ben Dhia, H., Wassim, A., 2012b. Groundwater evolution of the Continental Intercalaire aquifer of Southern Tunisia and a part of Southern Algeria: Use of geochemical and isotopic indicators. (Watmed6-Sousse September 2012-Tunisia).

Hamed, Y., Mokadem, N., Ben Dhia, H., 2012c. Hydrochemical changes induced by overexploitation of groundwater in North Africa: a case study of southern Gafsa basin (SW Tunisia). Annaba 20-22 Nov, 2012-Algeria.

Hamed, Y., Dhahri, F., 2013. Hydro-geochemical and isotopic composition of groundwater and meteoric water, with emphasis on sources of salinity, in the aquifer system in Northwestern Tunisia. Journal of African Earth Sciences. doi: 10.1006/s22517-013-0313-3.

Hamed, Y., Awad, S., Ben Sâad, A., 2013a. Nitrate contamination in groundwater in the Sidi Aïch-Gafsa Oasis region, Southern Tunisia. Journal: Environ Earth Sci. doi 10.1007/s12665-013-2445-5.

Hamed, Y., Mokadem, N., Ben Dhia, H., 2013b. Hydrochemical changes induced by overexploitation of groundwater in North Africa: a case study of southern Gafsa basin (SW Tunisia). Annaba 20-22 Nov-Algeria.

Hamed, Y., Hadj, R., Mokadem, N., 2013c. The Continental Intercalaire groundwater salinization in Southern Tunisia. 3rd International Symposium. Geoscience in the Service of Sustainable Development. 18-19 November. Tebessa-Algeria.

Hamed, Y., Al-Gamal, S.A., Ali, W., Nahid, A., Ben Dhia, H., 2013d. Palaeoenvironments of the Continental Intercalaire fossil from the Late Cretaceous (Barremian-Albian) in North Africa: a case study of southern Tunisia. Arab J Geosci. doi 10.1007/s12517-012-0804-2.

Henchiri and S'Himi, 2006. Silicification of sulphate evaporates and their carbonate replacements in Eocene marine sediments, Tunisia: two diagenic trends. Sedimentology: 125.

Hoffmann, G., Jouzel, J., Masson, V., 2000. Stable water isotopes in atmospheric general circulation models. Hydrological Processes, 14, 1385-1406.

Jedoui, Y., Kallel, K., Labeyrie, L., Reyss, J.L., Montacer, M., Michel Fontugne, M., 2001. Variabilité climatique rapide lors du dernier Interglaciaire (stade isotopique marin 5e), enregistrée dans les sédiments littoraux du Sud-Est tunisien. Abrupt climatic variability of the Last Interglacial (marine isotopic 5e substage) recorded in the coastal sediments of southeastern Tunisia. Comptes Rendus de l'Académie des Sciences - Series IIA - Earth and Planetary Science. Volume 333, Issue 11, 15 December, 2001, Pages 733-740.

Kamel, S., Dassi, L., Zouari, K., Abidi, B., 2005. Geochimical and isotopic investigation of the aquifer system in the Djerid-Nefzaoua basin, southern Tunisia. Eviron. Geol. 49, 159-170.

Kirchner, J.O.G., 1994. Investigation into the contribution of ground water to the salt load of the Breede River, using natural isotopes and chemical tracers. Report No. 344/1/95. Water Research Commission, Pretoria.

Kamel, S., 2012. Application of selected geothermometers to Continental Intercalaire thermal water in southern Tunisia. Geothermics 41. 63-73.

Kallel, N., Paterne, M., Duplessy, J.C., Vergnaud-Grazzini, C., Pujol, C., Labeyrie, L., Arnold, M., Fontugne, M., Pierre, C., 1997a. Enhanced rainfall in the Mediterranean region during the last sapropel event. Oceanologica Acta 20, 697-712.

Mokadem, N., Hamed, Y., Ben Sâad, A., Gargouri, I., 2012. Atmospheric pollution in North Africa (Ecosystems Atmosphere interactions): A case study in the mining basin of El

Guettar-M'Dilla (Southwestern Tunisia). Arabian Journal of Geosciences. doi: 10.1007/s12517-013-0852-2.

Mokadem, N., Hamed, Y., Bouri, S., Ben Dhia, H., 2013a. Overexploitation of groundwater and the extinction of springs systems: a case study in mining Gafsa basin (SW of tunisia). The 5th Tunisian days of applied geology: (Hammamt 17-20 mai 2013).

Mokadem, N., Younes, H., Hfaid, M., Ben Dhia, H., 2013b. Hydrogeochemical and isotope evidence of groundwater evolution in El Guettar oasis area, Southwest Tunisia (accepted).

Mokaddem, N., Demdoum, A., Redhaounia, B., Hamed, Y., Bouri, S., 2014. Étude géochimique et isotopique des eaux souterraines du bassin de Gafsa nord sud-ouest de la Tunisie. Quatrième Forum de l'Eau, Sousse, Tunisie, du 24 au 26 Mars 2014.

Mamou, A., 1990. Caractéristiques et évaluation des ressources en eau du Sud tunisien; Thèse Doct. Etat ès Sc. Univ. Paris Sud, centre d'Orsay, p. 403.

Mc Lean., Jankowski, W., J., Lavitt, N., 2000. Groundwater quality and sustainability in alluvial aquifer, Australia. In Sililoo. Et (eds) Groundwater, past achievement and future challenges. A. A. Bolkema, Rotterdam, Netherlands.

M'Rabet, A., 1987. Stratigraphie, sédimentation et diagenèse carbonatées des séries du Crétacé inférieur de Tunisie centrale.Thése és.Sci., Ann.Mines et géol., 30,385p.

Maliki, M.A., 2000. Etude hyrogéologique, hydrochimique et isotopique du système aquifère de Sfax (Tunisie). Doc Thesis, Tunis II University, Tunis, Tunisia.

OSS, 2003. Système Aquifère du Sahara Septentrional. Observatoire du Sahara et du Sahel. Tech. Rep. 9973-856, Tunis.

OSS, 2008. The North-Western Sahara Aquifer System: Concerted Management of Transboundary Water Basin. Sahara and Sahel Observatory, 48 pp.

Ouda, B., 2000. Paléohydrologie isotopique du basin de Meknassi (Tunisie centrale) pendant le quaternaire recent Paleohyrology.

Outtani, F., Addoum, B., Mercier, E., Frizon, D L., Andrieux, J., 1995. Geometry and kinematics of the south Atlas front, Algeria and Tunisia. Tectonophysics, 249, 233-248.

Ophori, D.U., Toth, J., 1988. Patterns of ground-water chemistry, Ross Creek Basin, Alberta, Canada. Ground Water 27 (1), 20-55.

Ounis, A., Lavanchy, J.C., Pfeifer, H.R., Chaabani, F., 2006. Etude Minéralogique et géochimique de la série phosphatée principale dans la partie occidentale du bassin de Gafsa Métlaoui.16ème journée des sciences Biologique et Environnement, 4-7 Nov. Tunisie.

Piper, A.M., 1944. A graphic procedure in the geochemical interpretation of water analyses. Trans. Am. Geophys. Union 25, 914-923.

Plummer, L.N., Prestemon, E., Parkhurst., D.L., 1992. An interactive code (netpath) for modelling net geochemical reactions along a flow path. USGS Water Resour. Inv. Rep. 91-4078, US Geological Survey.

Rozanski, K., Araguas, L., Gonfiantini, R., 1993. Isotopic patterns in modern global precipitation. In: Continental Isotope Indicators of Climate. American Geophysical Union (monograph).

Rouabhia, A., Baali, F., Kherici, N., Djabri, L., 2004. Vulnérabilité et risque de pollution des eaux souterraines de la nappe des sables miocènes de la plaine d'El MA EL Abiod (Algérie), Revue Sécheresse Vol.15, n°4.

Rouabhia, A., Baali, F., Fehdi, Ch., Kherici, N., Djabri, L., 2008a. Hydrochemical and isotopic investigation of a sandstone aquifer groundwater in a semi arid region, El Ma El Abiod, Algeria. Journal of Environmental Geology (Springer) Environ Geol. n°254. doi: 10.1007/s00254-008-1451-5.

Rouis-Zargouni, I., Turon, J.L., Londeix, L., Essallami, L., Kallel, N., Sicre, M.A., 2010. Environmental and climatic changes in the central Mediterranean Sea (Siculo-Tunisian strait) during the last 30 ka based on dinoflagellate cyst and planktonic foraminifera assemblages. Palaeogeogr. Palaeoclimatol. Palaeoecol. 285, 17-29.

Rogers, R.J., 1989. Geochemical comparison of groundwater in areas of New England, New York, and Pennsylvania. Groundwater 27 (5), 690-712.

Rindsberger, M., Magaritz, M., Carmi, I., Gilad, D., 1983. The relation between air mass trajectories and the water isotope composition in the Mediterranean Sea area. Geophysical Review Letters 10, 43-46.

Swezey, C., 2003. The role of climate in the creation and destruction of continental stratigraphic records : an example from the northern margin of the Sahara desert. SEPM (Society for Sedimentary Geology). Special Publication 77: 207-225.

Souayed, M., 1995. Dynamique de la sédimentation et modèle de dépôt des grès de Barrémien–Aptien en Tunisie septentrionale. Thèse. Université de Tunis II, 227p.

Soyer, C., Tricart, P., 1987. La crise aptienne en Tunisie centrale, approche paleo-structurale aux confins de l'Atlas et de l'Axe Nord-Sud. C.R. Acad. Sci. Paris II, 301-305.

Sonntag, C., Klitzsch, E., Lohnert, E.P., El-Shazly, E.M., Mijnnich, K.C., Junghans, C., Thorweihe, U., Weitroffer, K., Swailem, F.M., 1978. Paleoclimatic information from deuterium and oxygen-18 in Carbon-14-dated north Saharian groundwaters. In: isotope hydrology, vol II, IAEA-SM-228, (28), pp 569-581.

UNESCO., 1972. Etude des ressources en eau du Sahara Septentrional. Tech. Rep. 6 : pp. 44.

Ward, M.H., Mark, S.D., Cantor, K.P., Weisenburger, D.D., Correa-Villaseñor, A., Zahm, S.H., 1996. Drinking water nitrate and the risk of non-Hodgkin's lymphoma. Epidemiology 7, 465-471.

Weyer, P.J., Cerhan, J.R., Kross, B.C., Hallberg, G.R., Kantamneni, J., Breuer, G., Jones, M.P., Zheng, W., Lynch, C.F., 2001. Municipal drinking water nitrate level and cancer risk in older women: the Iowa women's health study. Epidemiology 12, 327-338.

WHO., 2006. World Health Organization. Guidelines for drinking water quality, 3rd edn, incorporating first addendum. Available at. http://www.who.int/water_sanitation_health/dwq/gdwq3rev/ en/index.html.

Wick, K., Heumesser, Ch., Schmid, E., 2012. Groundwater nitrate contamination: Factors and indicators. Journal of Environmental Management 111 (2012) 178-186.

Yermani, M., 2000. Etude hydrogéologique, hydrochimique et isotopique du bassin de Gafsa Nord. Doc Thesis, Tunis II University, Tunis, Tunisia.

Yermani, M., Zouari, K., Michelot, J.L., Mamou, A., Moumni, L. 2002. Approche géochimique du fonctionnement de la nappe profonde de Gafsa Nord (Tunisie centrale) /Geochemical approach to the functioning of the Gafsa North deep aquifer (central Tunisia). Hydrol. Sci. J. 48 (1), 95-108.

Zouaghi, T., Bédir, M., Abdallah, H., Inoubli, M.H., 2009. Seismic sequence stratigraphy, basin structuring, and hydrocarbon implications of Cretaceous deposits (Albian-Maastrichtian) in central Tunisia. Cretaceous Research 30, 1-21.

Zouaghi, T., Rihab, Guellala, R., Lazzez, M., Bédir, M., Ben Youssef, M., Inoubli, M.H., Zargouni, F., 2011. The Chott Fold Belt of Southern Tunisia, North African Margin: Structural Pattern, Tectono-Sedimentary, and Regional Geodynamic Implications. “New Frontiers in Tectonic Research-At the Midst of Plate Convergence”. Intech-Book, Vienna, Austria; ISBN: 978-953-307-594-5, pp. 49-72.

Zouari, K., Chkir, N., Ouda, B., 2003. Paleoclimatic variation in Maknassi basin (central Tunisia) during Holocene period using pluridisplinary approaches. IAEA, Vienna. CN. 28-80.

Zargouni, F., 1985. Tectonique de l'Atlas méridional de Tunisie. Evolution géométrique et cinématique des structures en zones de cisaillement. Thèse, Doctorat es Sciences, Université de Louis Pasteur de Strasbourg, France. pp. 306.

Zuppi, G.M., Sacchi,, E., 2004. Hydrogeology as a climate recorder: Sahara–Sahel (North Africa) and the Po Plain (Northern Italy). Global and Planetary Change 40, 79-91.

Zouari, H., Turki, M.M., Delfeil, J., 1990. Nouvelles données sur l'evolution tectonique de la chaïne de Gafsa. Bull. Soc. GEol. Fr., 8, VI: 621-629.

List of figures

Fig. 14. Plot of $\delta^{18}O$/Cl diagram.

List of tables

Table 1.

N°	Aquifer	Na	Ca	Mg	K	HCO_3	SO_4	Cl	NO_3	ER	$\delta^{18}O$	$\delta^{2}H$	d
		(meq/l)								(%)	(‰ *versus* SMOW)		
1	MPQ	20.27	5.43	15.41	0.76	1.94	22.73	20.95	0.04	-4.33	-7	-53	3
2	MPQ	19.62	18.52	8.76	0.81	1.95	23.1	22.44	0.04	0.21			
3	MPQ	14.54	21.49	9.85	1.08	1.92	21.92	18.7	0.37	4.51	-5.1	-40	0.8
4	MPQ	20.35	20.6	10.33	0.82	1.94	24.79	24.57	0	0.76			
5	MPQ	17.8	18.42	8.97	0.74	1.9	21.26	20.8	0.01	2.18	-5.2	-56	-14.4
6	MPQ	14.45	15	6.24	0.75	1.92	14.59	15.3	0.05	6.71	-6.2	-39	10.6
7	MPQ	26.19	22.78	10.38	0.93	1.95	25.87	31.73	0.05	0.57			
8	MPQ	5.36	6.91	5.1	0.1	1.97	9.3	5.1	0.07	3.05	-7.1	-60	-3.2
9	MPQ	7.94	5.7	5.33	0.1	1.87	10.36	5.38	0.34	2.99	-6	-49	-1
10	MPQ	1.41	5.33	2.3	0.02	1.94	7.06	0.86	0.23	-5.29	-5.3	-38	4.4
11	MPQ	2.9	4.56	2.96	0.05	1.93	6.92	1.24	0.23	0.73			
12	MPQ	3.7	6.32	4.1	0.05	1.91	9.43	2.21	0.35	0.95			
13	MPQ	5.03	9.1	5.05	0.05	1.92	12.43	3.13	0.56	3.19			
14	MPQ	4.03	9.74	4.36	0.05	1.96	11.5	2.6	0.36	5.09	-4.9	-41	-1.8
15	MPQ	4.34	8.66	4.99	0.04	1.97	10.95	3.17	0.56	4			
16	MPQ	3.29	7.86	3.23	0.04	1.92	8.65	1.83	0.24	6.58			
17	MPQ	5.31	10.31	3.27	0.02	1.93	11.92	2.54	0.14	6.72			
18	MPQ	3.25	7.79	2.98	0.03	1.92	8.64	1.78	0.37	4.99	-5.3	-38	4.4
19	MPQ	3.67	4.88	2.83	0.04	1.95	8.64	1.78	0.37	-5.47			
20	MPQ	3.69	1.75	10.75	0.04	1.94	9.84	1.68	0.38	7.92	-5.1	-39	1.8
21	MPQ	3.79	1.8	8.53	0.03	1.92	9.66	1.7	0.3	2.08			
22	MPQ	4.62	8.45	3.04	0.06	1.97	11.73	1.64	0.25	1.84			
23	MPQ	2.43	6.01	6.44	0.07	1.9	10.17	1.66	0.21	3.53			
24	MPQ	4.82	11.86	4.82	0.05	1.91	12.17	4.71	0.25	6.2	-4.9	-37	2.2
25	MPQ	5.39	4.18	6.2	0.05	1.92	12.98	3.71	0.53	-9.44	-5.7	-43	2.6
26	MPQ	9.02	5.86	17.03	0.11	1.93	21.3	6.65	0.68	2.32			
27	MPQ	9.2	10.51	10.82	0.14	1.95	24.59	6.02	1.08	-4.6			
28	MPQ	7.42	8.51	9.12	0.12	1.9	18.92	5	0.63	-2.45			
29	MPQ	7.34	13.43	17.49	0.12	1.95	29.15	7.82	0.77	-1.68			
30	MPQ	8.87	9.3	11.2	0.11	1.93	25.96	7.68	0.58	-10.15			
31	MPQ	8.97	8.81	11.03	0.12	1.95	24.42	8.61	0.54	-10.23			
32	MPQ	9.61	8.34	9.06	0.12	1.97	20.77	6.15	0.36	-3.76			
33	MPQ	16.32	13.59	15.12	0.15	1.93	32.16	13	0.3	-2.37			
34	MPQ	21.37	16.46	20.15	0.18	1.95	42.47	19.1	0.42	-4.72			
35	MPQ	28.48	18.19	24.06	0.16	1.94	44.9	30.19	0.47	-4.45			
36	MPQ	35.8	18.21	52.43	0.2	1.9	55.75	41.69	0.48	3.3			
37	MPQ	20.06	14.11	16.86	0.14	1.95	33.54	19.1	1.19	-4.3			
38	MPQ	20.38	15.8	19.96	0.16	1.9	40.18	20.96	1.47	-6.79			
39	MPQ	4	4.44	3.31	0.05	1.94	5.94	3.32	0.59	0.09			
40	MPQ	5.76	3.48	1.9	0.04	1.93	7.02	2.77	0.3	-3.6			
41	MPQ	3.7	4.66	3.27	0.05	1.95	6.71	2.59	0.21	0.93			
42	MPQ	4.67	4.92	3.63	0.07	1.94	7.9	3.32	0.39	-0.96			
43	MPQ	11.93	8.89	10.18	0.14	1.95	16.16	14.3	0.2	-2.28			
44	MPQ	14.99	11.59	13.24	0.15	1.93	22.76	17.43	0.31	-2.97			
45	MPQ	18.32	7.01	19.38	0.13	1.93	18.59	16.97	0.32	8.49			
46	UC	3.73	4.98	4.1	0.06	1.94	7.39	2.96	0.27	1.19	-6.4	-47	4.2
47	UC	5.1	5.58	5.08	0.1	1.92	9.09	4.06	0.28	1.67			
48	UC	3.95	5.53	4.73	0.07	1.91	7.58	4.16	0.15	1.69			
49	UC	3.9	5.5	4.7	0.06	1.89	8.12	4.1	0.15	-0.32			
50	UC	2.49	4.43	2.38	0.05	1.94	6.03	1.42	0.4	-2.27			
51	UC	6.23	4.44	2.76	0.06	1.94	8.02	3.81	0.44	-2.55			
52	UC	1.85	3.25	4.01	0.07	1.92	7.34	1.8	0.37	-10.88			
53	UC	4.58	5.98	4.4	0.12	1.87	7.71	4.92	0.13	1.49	-6.9	-50	5.2
54	UC	3.5	5.42	4.29	0.07	1.9	9.05	1.67	0.28	1.4	-5.9	-41	6.2
55	UC	10.27	4.93	5.84	0.13	1.93	12.32	4.62	0.48	4.47			
56	UC	27.07	15.91	23.76	0.16	1.93	20.48	26.93	0.62	14.48			
57	UC	16.89	11.53	14.95	0.12	1.89	10.84	13.6	0.49	23.72			
58	UC	14.95	10.3	10.98	0.1	1.93	18.85	9.37	0.3	8.8			
59	UC	15.84	7.06	14.8	0.1	1.97	18.59	10.77	0.28	8.9			
60	UC	14.72	6.61	16.82	0.1	1.92	18.2	10.32	0.27	10.91			
61	UC	14.23	9.63	11.53	0.18	1.91	17.8	9.69	0.24	9.09			
62	UC	13.75	6.81	14.68	0.17	1.94	16.92	9.75	0.27	10.14			
63	UC	13.15	6.88	13.55	0.15	2.01	17.23	9.11	0.27	8.18			
64	UC	12.44	6.59	13.91	0.15	1.97	16.42	8.62	0.27	9.6			
65	UC	12.28	6.44	13.55	0.14	1.93	15.92	8.21	0.27	10.34			
66	UC	12.33	5.61	14.1	0.11	1.92	15.55	8.08	0.24	10.96			
67	UC	11.02	6.08	14.36	0.1	1.95	15.24	7.93	0.29	10.78			
68	UC	7.12	5.91	15.08	0.1	1.99	14.96	7.8	0.32	5.87			
69	UC	6.94	5.64	14.75	0.1	1.95	14.84	7.78	0.46	4.56			
70	UC	7.08	8.78	8.02	0.1	1.95	14.65	7.63	0.68	-1.89			
71	UC	6.5	9.01	8.61	0.13	1.9	14.47	8.44	0.79	-2.68			
72	UC	7.11	8.79	6.75	0.12	1.92	14.41	7.11	0.4	-2.26			
73	UC	7.86	9.52	7.46	0.11	1.95	14.65	8.22	0.52	-0.77			
74	UC	8.7	8.94	8.22	0.12	1.95	17.05	8.82	0.34	-4.02			
75	UC	6.63	8.46	7.57	0.1	1.93	13.73	7.45	0.66	-2.19			
76	UC	14.51	10.04	12.76	0.15	1.97	26.61	11.14	0.99	-4.14			
77	UC	26.61	17.44	12.83	0.53	1.92	38.28	24.01	0.06	-5.63			
78	UC	12.23	7.13	19.95	0.14	1.94	23.56	8.52	0.52	6.62			
79	UC	10.37	6.78	20.71	0.13	1.92	20.88	7.81	0.52	9.9			
80	UC	9.63	6.18	18.63	0.1	1.93	20.59	6.8	0.54	7.27			
81	UC	3.71	4.32	3.64	0.09	1.9	5.64	2.79	0.36	4.76			
82	UC	2.29	4.07	2.76	0.12	1.97	4.72	2.62	0.63	-3.64			
83	UC	6.94	3.03	1.92	0.06	1.96	5.94	3.93	0.48	-1.44			
84	UC	18.36	7.25	20.3	0.11	1.95	18.79	17.67	0.35	8.53			
85	LC	18.8	7.12	20.08	0.12	1.92	17.02	17.88	0.33	10.77			
86	LC	17.88	7.1	20.14	0.12	1.92	17.96	18.08	0.33	8.3			
87	LC	17.91	6.63	19.02	0.14	1.95	18.11	16.85	0.3	8.03			

Table 2.

N°	Aquifer	T	pH	EC	TDS	Saturation Index (SI)					
		(°C)		(mS/cm)	(g/l)	Halite	Gypsum	Anhydrite	Calcite	Dolomite	Aragonite
1	MPQ	23	6.83	4.21	2,89	-5.15	0.97	-1.19	-0.88	-0.89	-1.03
2	MPQ	23	7.63	4.12	2,72	-5.13	-0.38	-0.6	0.44	0.68	0.3
3	MPQ	23	7.84	5.02	3,24	-5.33	-0.34	-0.56	0.71	1.2	0.57
4	MPQ	23	7.51	4.34	2,91	-5.08	-0.33	-0.55	0.36	0.53	0.21
5	MPQ	23	7.64	3.98	2,58	-5.2	-0.4	-0.62	0.45	0.71	0.31
6	MPQ	23	7.43	3.16	2,06	-5.4	0.56	-0.78	0.22	0.18	0.08
7	MPQ	23	7.81	5.32	3,59	-4.87	-0.3	-0.52	0.67	1.12	0.53
8	MPQ	23	6.97	1.62	0,97	-6.27	-0.92	-1.14	-0.47	-0.95	-0.61
9	MPQ	23	7.13	1.64	1,04	-6.08	-0.97	-1.19	-0.43	-0.76	-0.57
10	MPQ	23	7.61	1.18	0,5	-7.6	-1.04	-1.26	0.11	-0.03	-0.04
11	MPQ	23	7.38	0.815	0,54	-7.13	-1.12	-1.34	-0.19	-0.45	-0.33
12	MPQ	23	7.66	0.812	0,8	-6.79	-0.92	-1.14	0.18	0.28	0.03
13	MPQ	23	7.18	1.32	1,17	-6.52	-0.72	-0.94	-0.18	-0.5	-0.32
14	MPQ	23	7.56	1.84	1,09	-6.69	-0.71	-0.93	0.24	0.25	0.1
15	MPQ	23	7.89	1.82	1,11	-6.58	-0.78	-1	0.52	0.92	0.38
16	MPQ	23	6.54	1.38	0,84	-6.92	-0.86	-1.08	-0.83	-1.93	-0.97
17	MPQ	23	7.38	1.79	1,12	-6.59	-0.68	-0.9	0.08	-0.22	-0.06
18	MPQ	23	7.65	1.38	0,86	-6.94	-0.86	-1.08	0.27	0.24	0.13
19	MPQ	23	8.89	1.33	0,83	-6.88	-1.04	-1.26	1.27	2.3	1.07
20	MPQ	23	7.79	0.81	0,59	-6.91	-1.5	-1.72	-0.25	0.4	-0.39
21	MPQ	23	7.94	1.88	1,25	-6.89	-1.46	-1.68	-0.09	0.61	-0.23
22	MPQ	23	8.02	1.03	0,74	-6.83	-0.74	-0.96	-0.63	0.94	-0.49
23	MPQ	23	7.68	1.33	0,92	-7.1	-0.94	-1.16	0.17	0.84	0.02
24	MPQ	23	7.49	1.18	0,56	-6.37	-0.64	-0.86	0.23	0.19	0.09
25	MPQ	23	6.94	1.86	1,3	-6.41	-1.02	-1.24	-0.76	-1.23	-0.9
26	MPQ	23	7.64	2.19	1,56	-5.97	-0.83	-1.05	0	0.57	-0.15
27	MPQ	23	8.22	3.246	2,3	-6.01	-0.53	-0.75	0.78	1.69	0.64
28	MPQ	23	7.55	2.623	1,85	-6.17	-0.66	-0.88	0.09	0.31	-0.06
29	MPQ	23	7.62	3.937	2,84	-6	-0.42	-0.64	0.29	0.8	0.14
30	MPQ	23	7.81	3.534	2,56	-5.92	-0.56	-0.78	0.33	0.85	0.19
31	MPQ	23	8.03	3.452	2,47	-5.86	-0.6	-0.82	0.53	1.27	0.39
32	MPQ	23	8.12	2.885	2,1	-5.97	-0.65	-0.87	0.62	1.39	0.48
33	MPQ	23	7.81	4.056	2,89	-5.45	-0.4	-0.62	0.44	1.05	0.3
34	MPQ	23	7.73	6.301	4,45	-5.18	-0.28	-0.5	0.4	0.99	0.25
35	MPQ	23	7.43	7.467	5,32	-4.87	-0.26	-0.48	0.13	0.49	-0.02
36	MPQ	23	6.89	9.964	7,04	-4.65	-0.29	-0.51	-0.46	-0.35	-0.61
37	MPQ	23	7.15	5.44	3,85	-5.2	-0.39	-0.61	-0.2	-0.2	-0.34
38	MPQ	23	7.42	6.452	4,55	-5.16	-0.31	-0.53	0.08	0.36	-0.07
39	MPQ	23	7.64	0.884	0,63	-6.57	-1.21	-1.43	0.06	0.11	-0.08
40	MPQ	23	7.46	0.904	0,65	-6.49	-1.22	-1.44	-0.24	-0.62	-0.38
41	MPQ	23	7.84	0.817	0,61	-6.71	-1.14	-1.36	0.24	0.51	0.13
42	MPQ	23	8.06	1.073	0,78	-6.51	-1.08	-1.3	0.84	0.95	0.34
43	MPQ	23	7.92	2.867	2,14	-5.51	-0.74	-0.95	0.48	1.13	0.33
44	MPQ	23	7.34	4.045	2,87	-5.35	-0.56	-0.78	-0.03	0.11	-0.18
45	MPQ	23	7.61	2.586	1,84	-5.27	-0.86	-1.08	0.04	0.63	-0.11
46	UC	23	7.51	1.02	0,65	-6.66	-1.1	-1.32	-0.04	-0.04	-0.18
47	UC	23	6.89	1.52	0,92	-6.39	-1.01	-1.23	-0.64	-1.2	-0.78
48	UC	23	6.74	1.47	0,76	-6.49	-1.06	-1.28	-0.77	-1.5	-0.92
49	UC	23	7.54	1.29	0,74	-6.5	-1.04	-1.26	0.01	0.06	-0.14
50	UC	23	7.64	0.928	0,61	-7.14	-1.17	-1.39	0.7	-0.01	-0.07
51	UC	23	7.59	1.98	0,43	-6.33	-1.11	-1.33	-0.02	-0.13	-0.17
52	UC	23	7.82	0.966	0,72	-7.17	-1.24	-1.46	0.09	0.39	-0.05
53	UC	23	7.34	1.14	0,81	-6.35	-1.03	-1.29	-0.16	-0.33	-0.3
54	UC	23	8.01	0.98	0,76	-6.93	-0.99	-1.21	0.46	0.93	0.31
55	UC	23	7.68	1.199	1,29	-6.04	-0.98	-1.2	0.05	0.28	-0.1
56	UC	23	7.64	0.213	3,29	-4.92	-0.57	-0.79	0.37	1.04	0.23
57	UC	23	8.13	3.02	1,73	-5.39	-0.84	-1.05	0.78	1.8	0.64
58	UC	23	7.92	4.47	2	-5.6	-0.63	-0.85	0.52	1.18	0.37
59	UC	23	6.99	1.02	0,84	-5.52	-0.81	-1.03	-0.55	-0.66	-0.69
60	UC	23	7.05	0.348	0,12	-5.57	-0.86	-1.08	-0.53	-0.53	-0.67
61	UC	23	7.84	3.06	1,97	-5.61	-0.68	-0.9	0.41	1.02	0.27
62	UC	23	7.68	1.338	3,15	-5.62	-0.85	-1.07	0.12	0.7	-0.02
63	UC	23	7.92	0.812	0,18	-5.67	-0.83	-1.05	0.37	-0.92	0.23
64	UC	23	7.81	2.812	2,84	-5.71	-0.86	-1.08	0.25	0.94	0.1
65	UC	23	8.06	1.013	0,33	-5.74	-0.88	-1.1	0.48	1.39	0.33
66	UC	23	7.64	0.867	0,19	-5.74	-0.94	-1.16	0.01	0.54	-0.13
67	UC	23	6.88	2.71	0,71	-5.8	-0.92	-1.14	-0.69	-0.9	-0.84
68	UC	23	6.78	0.793	0,47	-5.9	-0.93	-1.15	-0.79	-1.06	-0.93
69	UC	23	7.54	2.2	1,4	-6	-0.95	-1.17	-0.07	0.4	-0.21
70	UC	23	7.88	2.323	1,66	-6	-0.73	-0.95	0.46	1	0.32
71	UC	23	7.64	2.759	1,7	-5.99	-0.73	-0.95	0.23	0.56	0.09
72	UC	23	7.68	2.248	1,61	-6.03	-0.72	-0.94	0.27	0.53	0.12
73	UC	23	7.54	2.399	1,7	-5.92	-0.7	-0.92	0.16	0.34	0.02
74	UC	23	7.61	2.689	1,91	-5.85	-0.68	-0.9	0.19	0.45	0.04
75	UC	23	8.42	2.17	1,58	-6.04	-0.76	-0.98	0.95	1.97	0.81
76	UC	23	8.13	3.959	2,82	-5.55	-0.55	-0.77	0.66	1.54	0.52
77	UC	23	7.95	6.121	4,48	-4.98	-0.27	-0.49	0.64	1.26	0.5
78	UC	23	7.86	4.583	3,3	-5.74	-0.75	-0.97	0.27	1.11	0.13
79	UC	23	8.01	1.113	0,83	-5.84	-0.81	-1.03	0.41	1.41	0.26
80	UC	23	7.64	2.606	1,84	-5.93	-0.84	-1.06	0.02	64	-0.12
81	UC	23	7.38	0.817	0,6	-6.68	-1.23	-1.45	-0.21	-0.38	-0.35
82	UC	23	8.12	0.611	0,44	-6.9	-1.3	-1.52	0.52	1	0.38
83	UC	23	7.76	0.772	0,56	-6.26	-1.51	-1.56	0.02	-0.04	-0.13
84	UC	23	7.18	1.692	1,27	-5.25	-0.85	-1.07	-0.37	-0.18	-0.52
85	LC	23	7.53	5.509	4,04	-5.23	-0.89	-1.11	-0.03	0.5	-0.18
86	LC	23	7.67	1.518	1,11	-5.25	-0.87	-1.09	0.1	0.77	-0.05
87	LC	23	7.81	6.555	14	-5.28	-0.89	-1.11	0.21	1	0.07

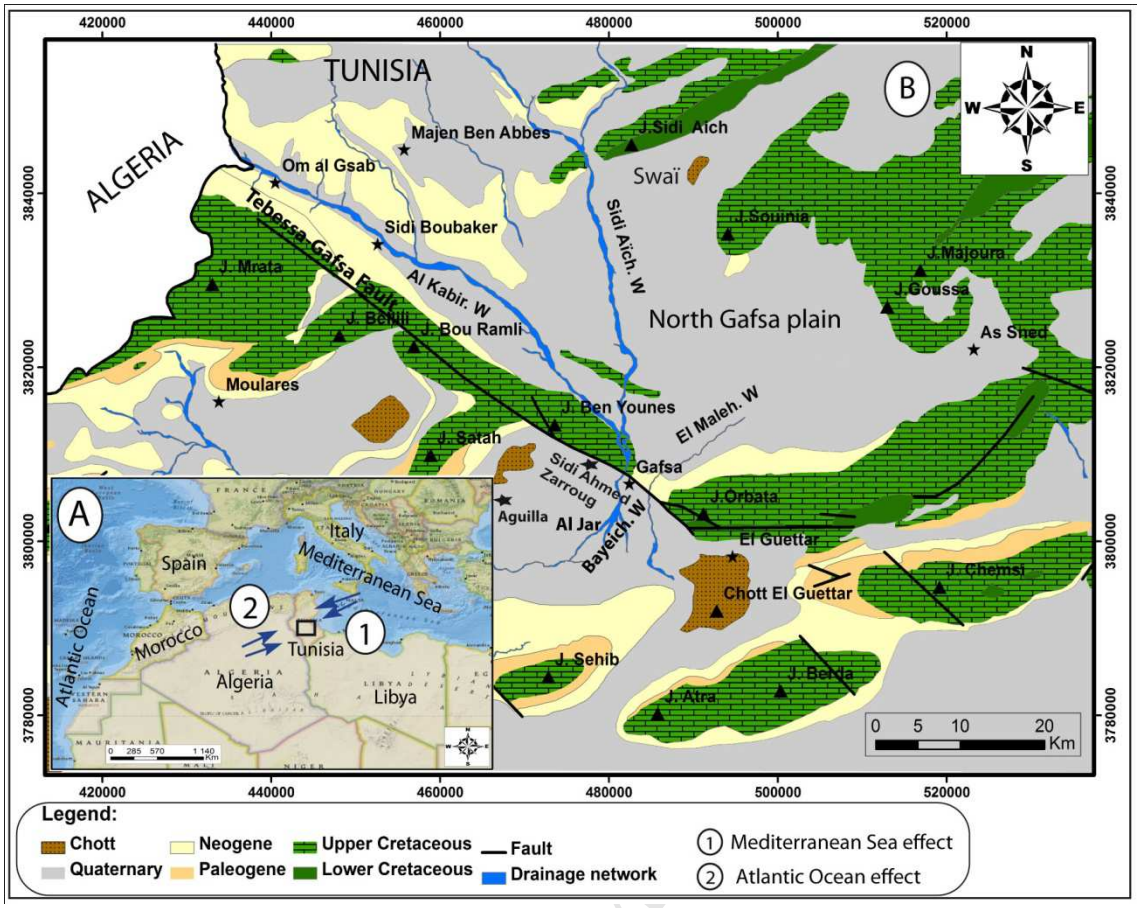

Fig. 1

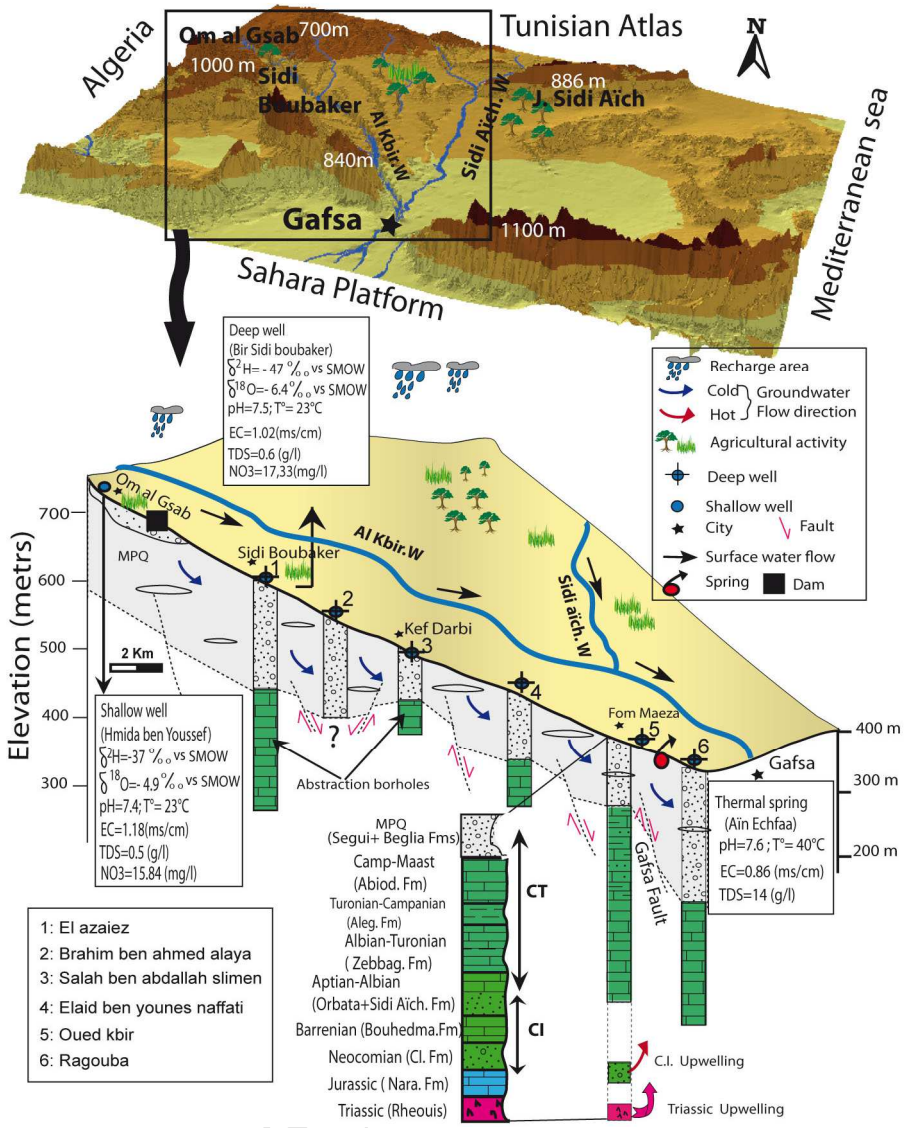
Algeria
Tunisian Atlas
N
Om al Gsab
700m
1000 m
Sidi Boubaker
Al Kbir.W
Sidi Aïch. W
886 m
J. Sidi Aïch
840m
Gafsa
1100 m
Sahara Platform
Mediterranean sea
Deep well
(Bir Sidi boubaker)
δ2H=- 47 ‰ vs SMOW
δ18O=- 6.4 ‰ vs SMOW
pH=7.5; T°= 23°C
EC=1.02(ms/cm)
TDS=0.6 (g/l)
NO3=17,33(mg/l)
Recharge area
Cold
Hot
Groundwater Flow direction
Agricultural activity
Deep well
Shallow well
City
Fault
Surface water flow
Spring
Dam
Elevation (metrs)
700
600
500
400
300
MPQ
2 Km
Kef Darbi
Fom Maeza
Gafsa
400 m
300 m
200 m
Shallow well
(Hmida ben Youssef)
δ2H=-37 ‰ vs SMOW
δ18O=- 4,9 ‰ vs SMOW
pH=7.4; T°= 23°C
EC=1.18(ms/cm)
TDS=0.5 (g/l)
NO3=15.84 (mg/l)
Abstraction borholes
Thermal spring
(Aïn Echfaa)
pH=7.6 ; T°= 40°C
EC=0.86 (ms/cm)
TDS=14 (g/l)
1: El azaiez
2: Brahim ben ahmed alaya
3: Salah ben abdallah slimen
4: Elaid ben younes naffati
5: Oued kbir
6: Ragouba
MPQ
(Segui+ Beglia Fms)
Camp-Maast
(Abiod. Fm)
Turonian-Campanian
(Aleg. Fm)
Albian-Turonian
(Zebbag. Fm)
Aptian-Albian
(Orbata+Sidi Aïch. Fm)
Barrenian (Bouhedma.Fm)
Neocomian (Cl. Fm)
Jurassic (Nara. Fm)
Triassic (Rheouis)
CT
CI
Gafsa Fault
C.I. Upwelling
Triassic Upwelling

Fig. 2

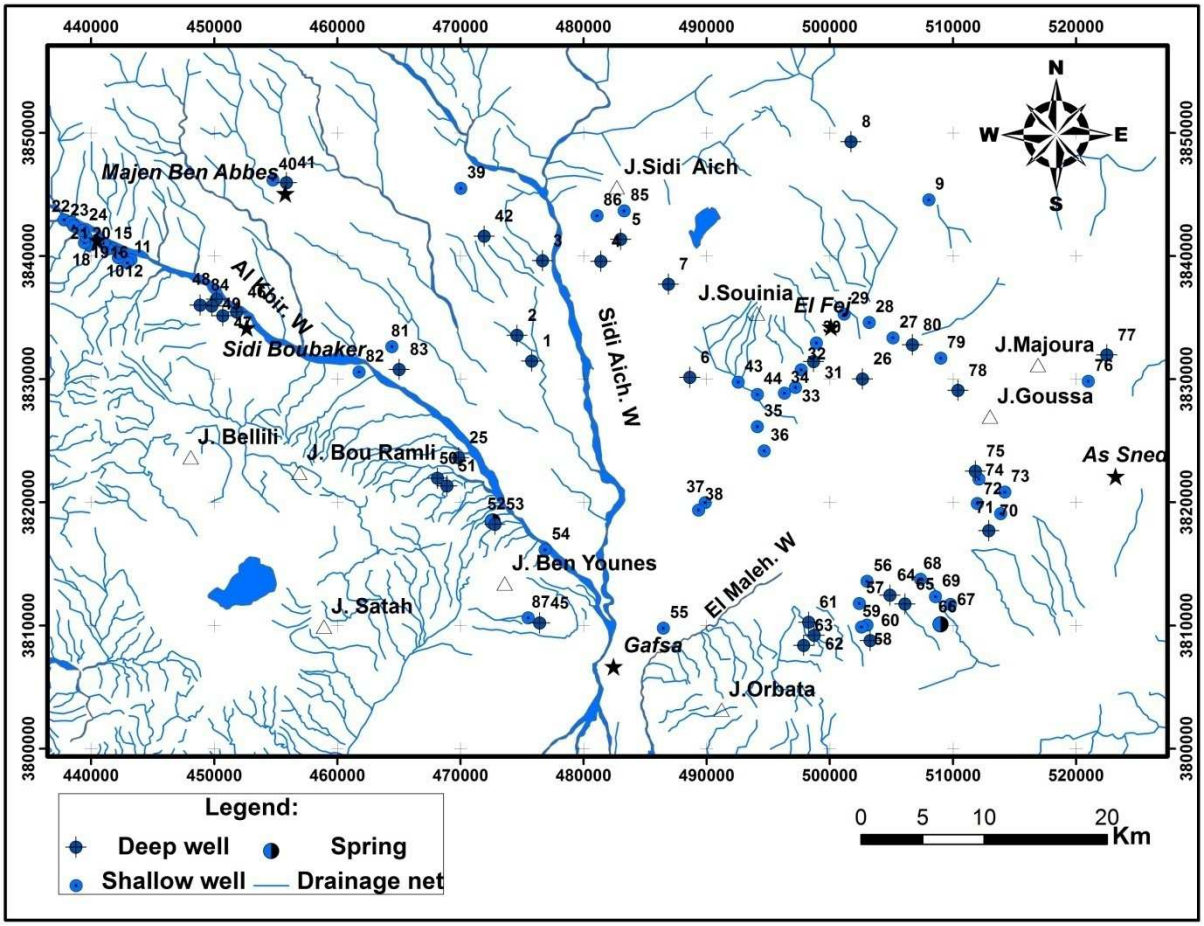

Fig. 3

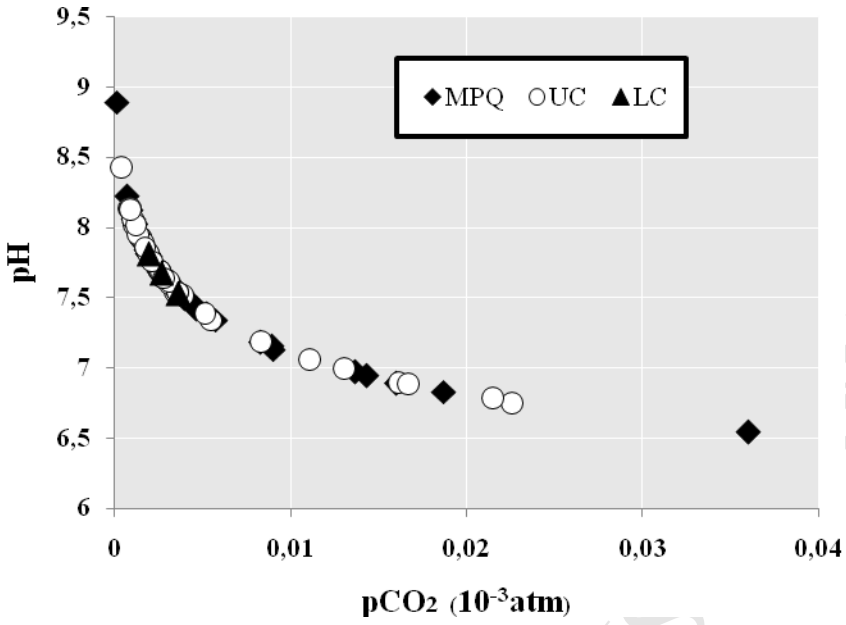

Fig. 4

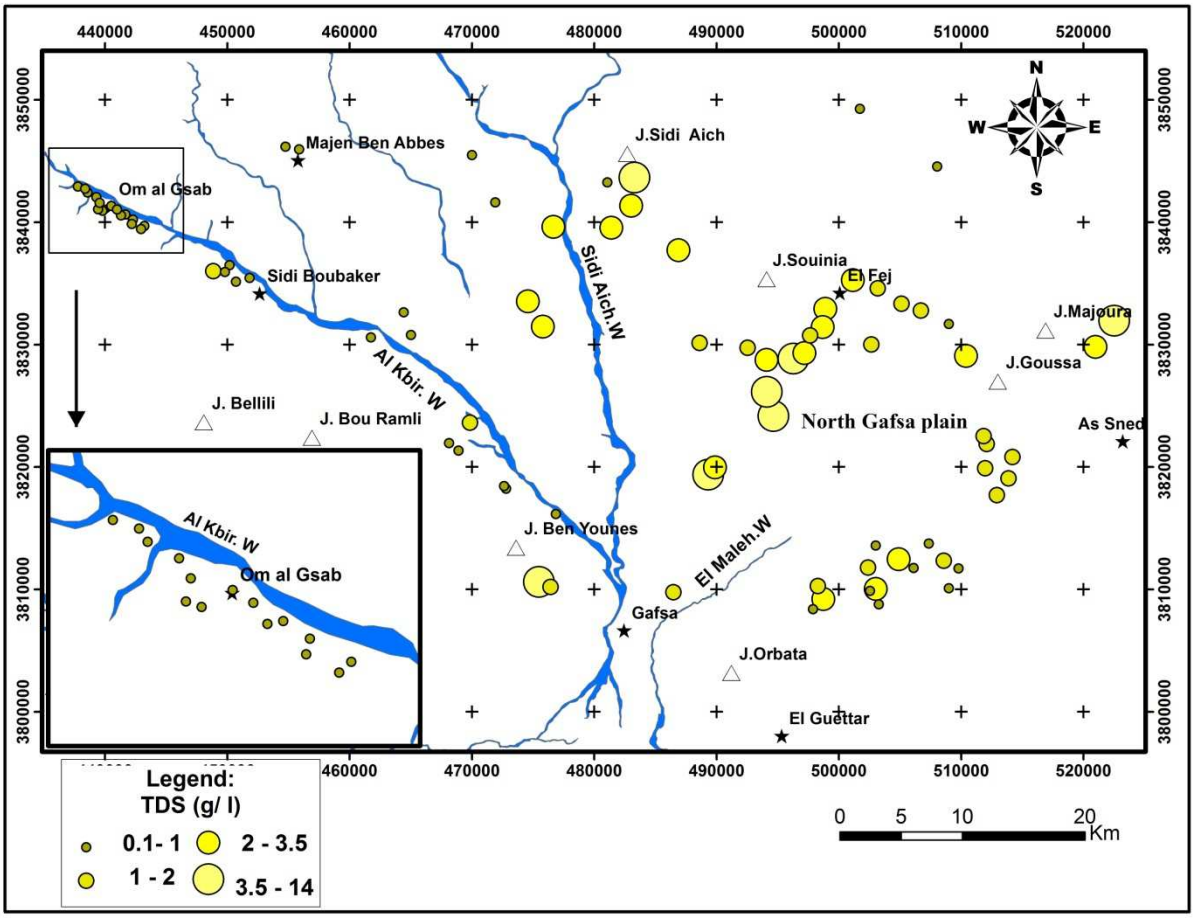

Fig. 5

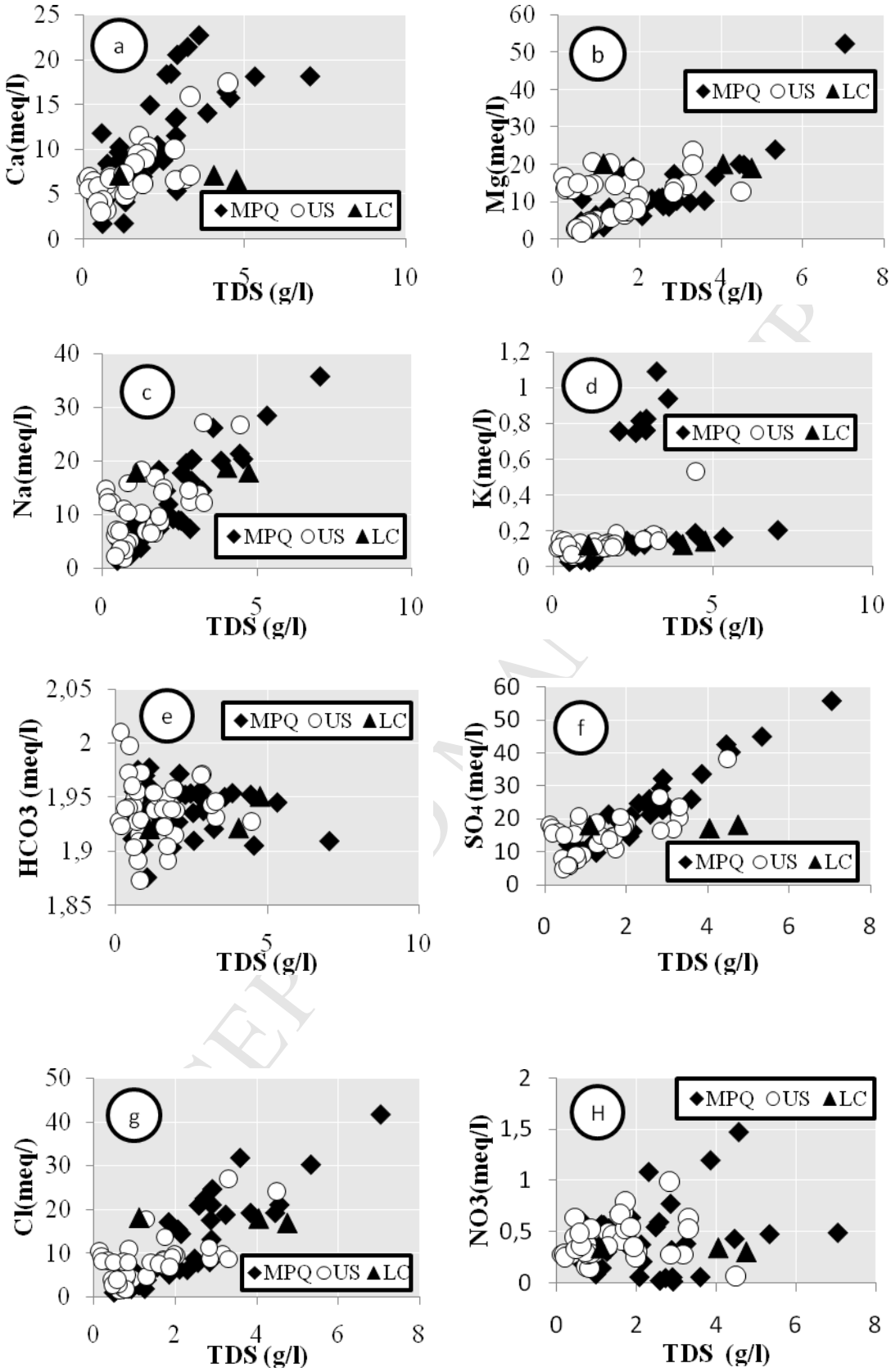
a
Ca(meq/l)
TDS (g/l)
◆MPQ ○US ▲LC
b
Mg(meq/l)
TDS (g/l)
◆MPQ ○US ▲LC
c
Na(meq/l)
TDS (g/l)
◆MPQ ○US ▲LC
d
K(meq/l)
TDS (g/l)
◆MPQ ○US ▲LC
e
HCO3 (meq/l)
TDS (g/l)
◆MPQ ○US ▲LC
f
SO4 (meq/l)
TDS (g/l)
◆MPQ ○US ▲LC
g
Cl(meq/)
TDS (g/l)
◆MPQ ○US ▲LC
H
NO3(meq/l)
TDS (g/l)
◆MPQ ○US ▲LC

Fig. 6

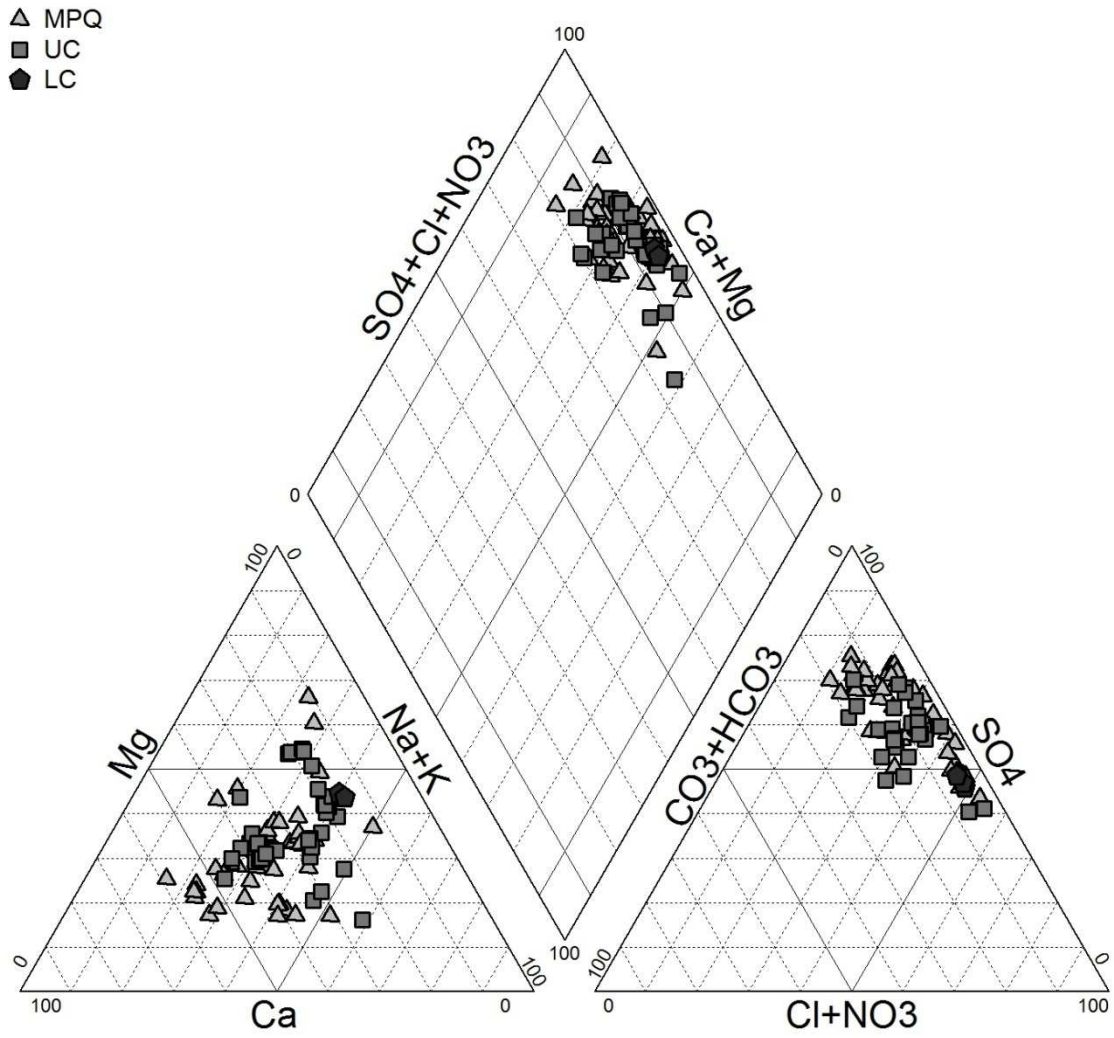

Fig. 7

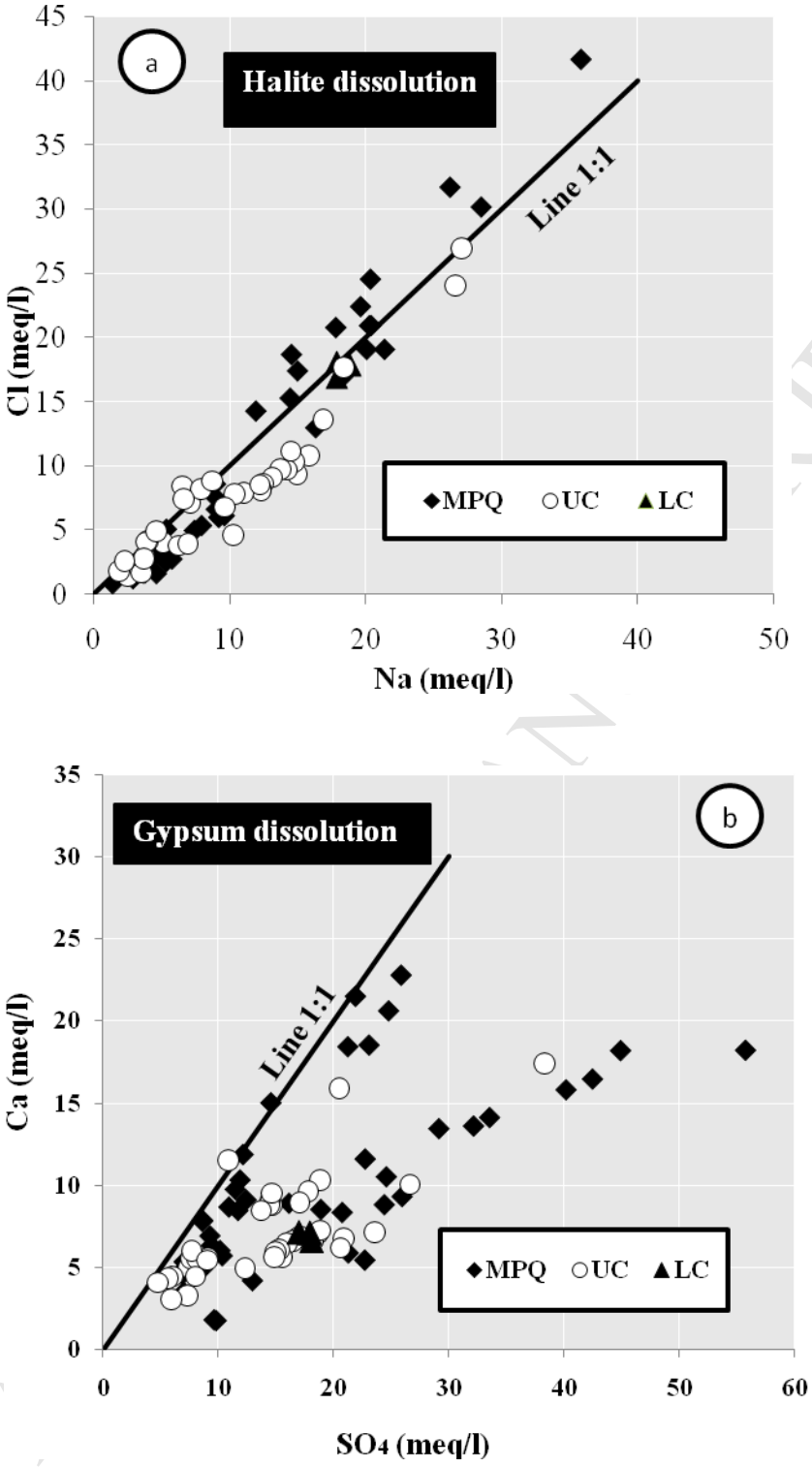
a
Halite dissolution
Line 1:1
MPQ
UC
LC
Cl (meq/l)
Na (meq/l)
0
5
10
15
20
25
30
35
40
45
0
10
20
30
40
50
b
Gypsum dissolution
Line 1:1
MPQ
UC
LC
Ca (meq/l)
SO4 (meq/l)
0
5
10
15
20
25
30
35
0
10
20
30
40
50
60

Fig. 8

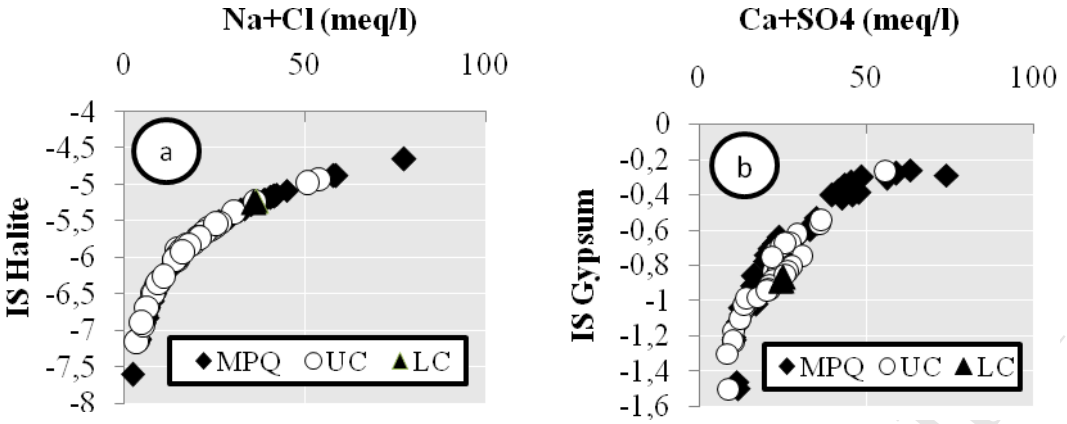
Na+Cl (meq/l)
0
50
100
-4
-4,5
-5
-5,5
-6
-6,5
-7
-7,5
-8
IS Halite
a
MPQ
UC
LC
Ca+SO4 (meq/l)
0
50
100
0
-0,2
-0,4
-0,6
-0,8
-1
-1,2
-1,4
-1,6
IS Gypsum
b
MPQ
UC
LC

Fig. 9

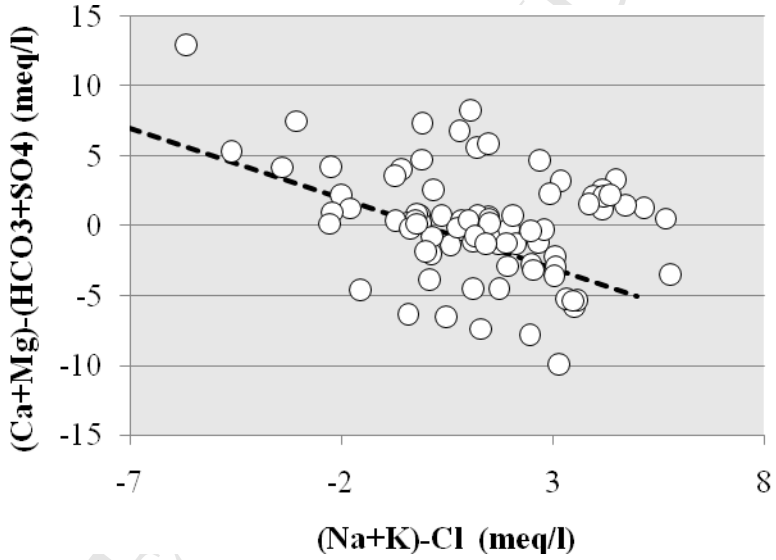
15
10
5
0
-5
-10
-15
(Ca+Mg)-(HCO3+SO4) (meq/l)
-7
-2
3
8
(Na+K)-Cl (meq/l)

Fig. 10

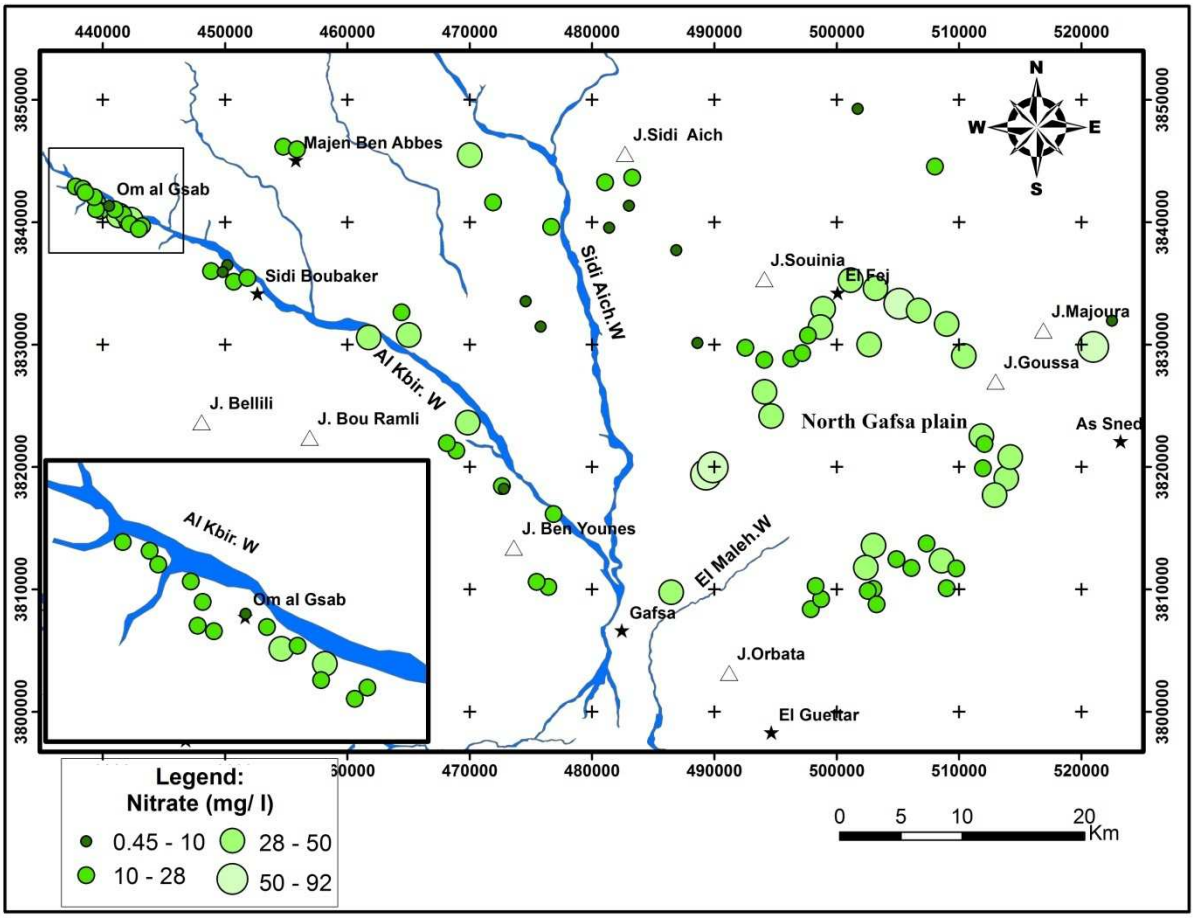

Fig. 11

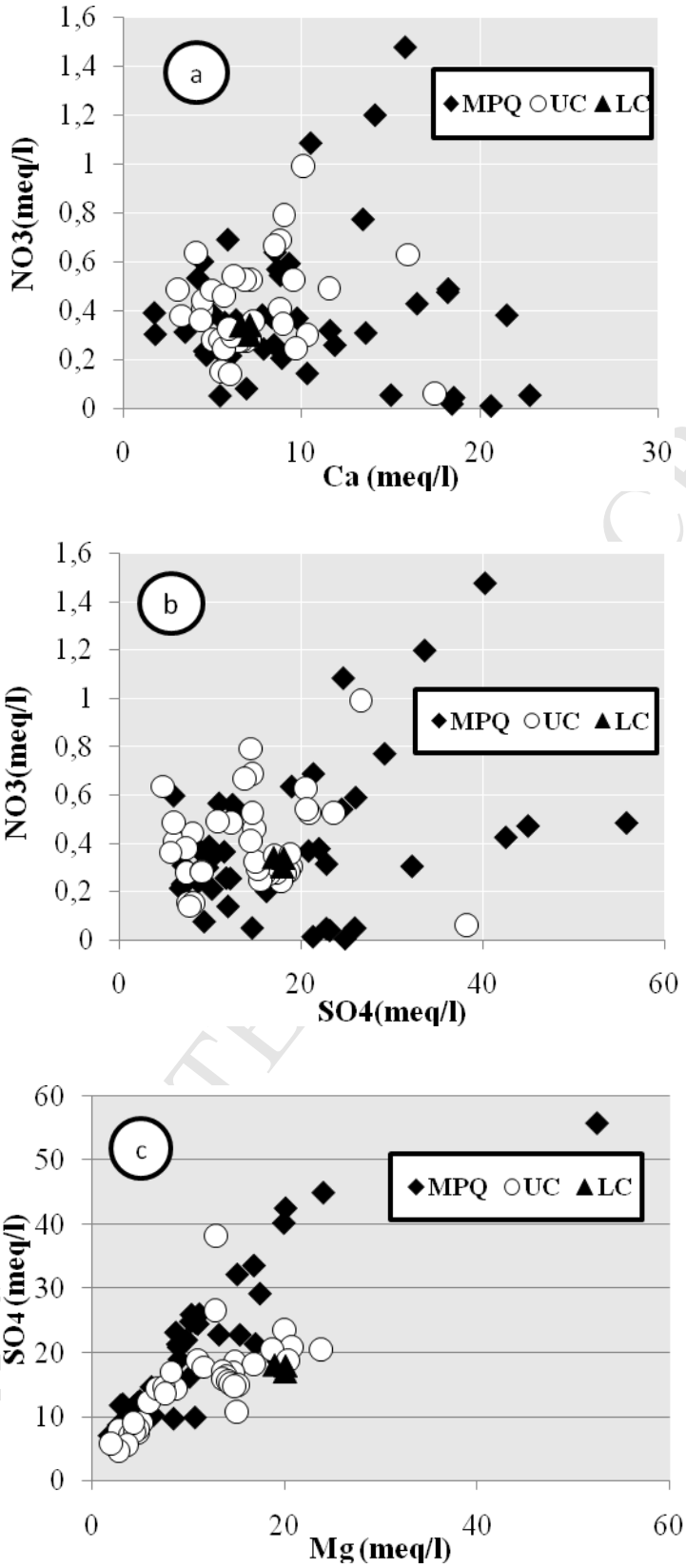
a
MPQ UC LC
NO3(meq/l)
Ca (meq/l)
b
MPQ UC LC
NO3(meq/l)
SO4(meq/l)
c
MPQ UC LC
SO4 (meq/l)
Mg (meq/l)

Fig. 12

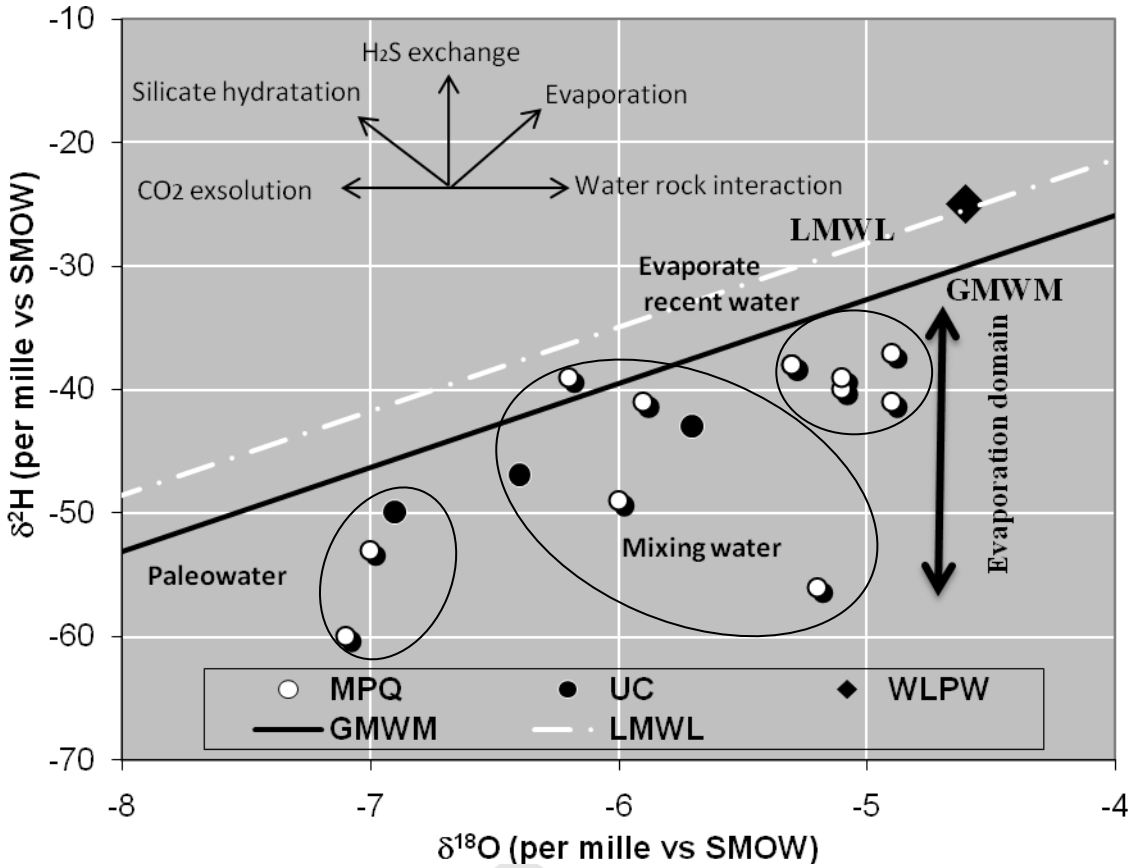

Fig. 13

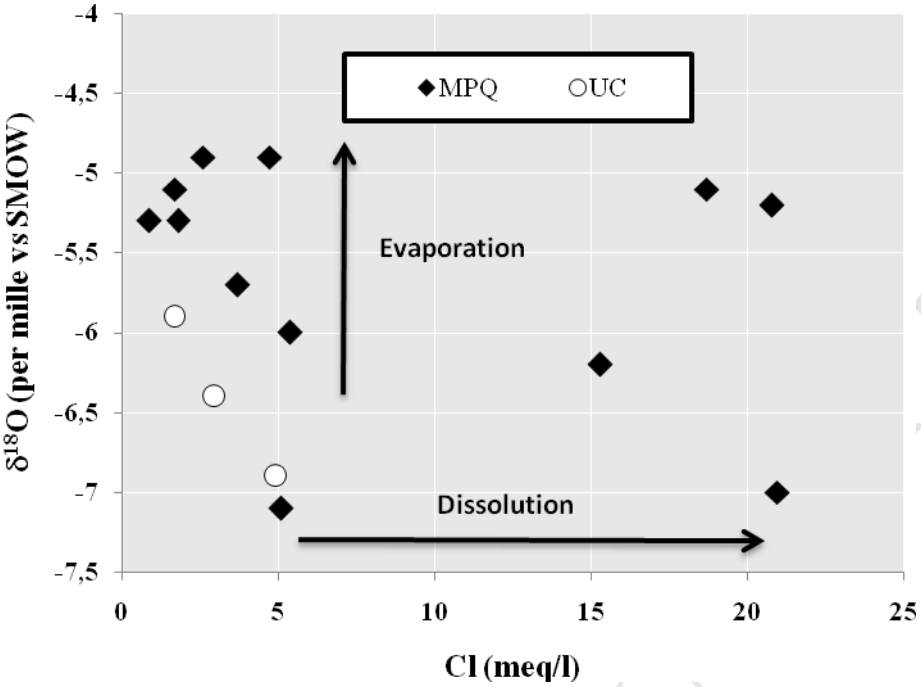

Fig. 14

Hydro and isotope geochemistry were used in this study:

- to identify the hydrodynamic functioning of the multi-aquifer system;
- to identify the inter-aquifer mixing;
- to investigate the water type of groundwater in the semi-arid southwestern Tunisia;